International Journal of Hydrogen Energy, Volume 47, Issue 10, February 2022, pp. 6586-6604
DOI:10.1016/j.ijhydene.2021.12.037

Techno-economic feasibility assessment of sorption enhanced gasification of municipal solid waste for hydrogen production

Mónica P. S. Santos and Dawid P. Hanak*

Energy and Power, School of Water, Energy and Environment,

Cranfield University, Bedford, Bedfordshire, MK43 0AL, United Kingdom.

*Corresponding author: *Dawid P. Hanak, d.p.hanak@cranfield.ac.uk*

Abstract

Waste-to-fuel coupled with carbon capture and storage is forecasted to be an effective way to mitigate the greenhouse gas emissions, reduce the waste sent to landfill and, simultaneously, reduce the dependence of fossil fuels. This study evaluated the techno-economic feasibility of sorption enhanced gasification, which involves in-situ CO_2 capture, and benchmarked it with the conventional steam gasification. of municipal solid waste for H_2 production. The impact of a gate fee and tax levied on the fossil CO_2 emissions in economic feasibility was assessed. The results showed that the hydrogen production was enhanced in sorption enhanced gasification, that achieved an optimum H_2 production efficiency of 48.7% (T=650 °C and SBR=1.8). This was 1.0% points higher than that of the conventional steam gasification (T=900 °C and SBR=1.2). However, the total efficiency, which accounts for H_2 production and net power output, for sorption enhanced gasification was estimated to be 49.3% (T=650 °C and SBR=1.8). This was 4.4% points lower than the figure estimated for the conventional gasification (T=900 °C and SBR=1.2). The economic performance assessment showed that the sorption enhanced gasification will result in a significantly higher levelised cost of hydrogen (5.0 €/kg) compared to that estimated for conventional steam gasification (2.7 €/kg). The levelised cost of hydrogen can be reduced to 4.5 €/kg on an introduction of the gate fee of 40.0 €/t_{MSW}. The cost of CO_2 avoided was estimated to be 114.9 €/tCO_2 (no gate fee and tax levied). However, this value can be reduced to 90.1 €/tCO_2 with the introduction of an emission allowance price of 39.6 €/tCO_2. Despite better environmental performance, the capital cost of sorption enhanced gasification needs to be reduced for this technology to become competitive with mature gasification technologies.

Keywords: Waste-to-fuel; modelling; waste management; hydrogen production; CO_2 capture

1. Introduction

Approximately two billion tonnes of municipal solid waste (MSW) are generated worldwide every year. It is forecasted that this figure can reach 3.4 billion tonnes by 2050 [1]. The MSW composition varies with the country's economic development, with the developing countries being responsible for the MSW with higher contents of organic matter [2]. The UK has reduced the biodegradable municipal waste sent to landfill from 7.4 million tonnes in 2017 to 7.2 millions of tonnes in 2018 [3]. However, in terms of greenhouse gas (GHG) emissions, these still corresponded to 14.4 million tonnes of CO_2 equivalent [4]. Therefore, waste-to-energy (WtE) or waste-to-fuel conversion is a promising route to reduce the amount of waste landfilled. Such processes also have the potential to support a reduction in GHG emissions, reducing the dependence on fossil fuels *via* the production of biofuels, power and/or heat. Therefore, the adoption of clean processes is of paramount importance with economic, environmental and health benefits [5].

Although H_2 production from different biomass feedstocks can be achieved *via* biological or thermochemical processes, the latter is most attractive as it offers faster process kinetics and leads to higher H_2 yields [6]. Among the main thermochemical routes, biomass gasification offers better results in terms of H_2 yield when compared with pyrolysis [7]. Biomass conversion into H_2 *via* gasification normally requires temperatures between 700 °C and 1200 °C and a gasifying agent, such as air [8], oxygen [9], steam [10] or CO_2 [11]. The use of pure oxygen rather than air leads to higher H_2 content and higher calorific value of the final product because there is no nitrogen dilution [12]. Steam gasification leads to even higher H_2 yields when compared with O_2 gasification. This can be attributed to the decomposition of water and the water gas shift (WGS) and methane reforming reactions[12]. The addition of steam also moves the equilibrium to the right enhancing the H_2 formation.

The products of biomass gasification are tars, chars and syngas. The typical syngas composition includes 30–50%$_{vol}$ of H_2, 25–40%$_{vol}$ of CO, 8–20%$_{vol}$ of CO_2 and 6–15%$_{vol}$ of CH_4, [13]. The composition and the H_2 yield depend on the biomass characteristics, gasification operating conditions, use of catalysts and reactor design configurations [6]. It needs to be emphasised that the formation of undesired by-products, such tars and inorganic impurities (H_2S, NH_3 and HCL), is the key drawback of biomass gasification. However, the content of tars, which increase the risk of fouling and blockage in the pipelines and equipment, can be reduced by introducing a catalyst such as Ni nanoparticles embedded carbon nanofiber/porous carbon [14], perovskite [15] or CaO [16]. Zhang et al. [14] have found that the use Ni nanoparticles embedded carbon nanofiber/porous carbon enhanced the tar conversion efficiency to 94.78% at 700 °C. Umar et al. [15] have shown that perovskite dopped with nanoparticles alkaline metals can be an effective catalyst on steam reforming of glycerol for H_2 production. Besides, this catalyst has proven to contribute to the fouling reduction. Jordan and Akay [16] have compared the syngas composition for the process with and without CaO and concluded that H_2 concentration increased from 12.1%$_{vol}$ to 16.5%$_{vol}$ without and with 6%$_{wt}$ CaO, respectively.

Furthermore, the carbon nanotubes supported Pt-bimetallic catalysts with CaO have proven to be an effective catalyst for H_2 production from sorption enhanced aqueous phase reforming of glycerol [18]. Since the WGS reaction is favoured in detriment to methanation reaction, the H_2 yield increases and the CH_4 yield reduces.

Importantly, calcium oxide (CaO) is regarded as a promising catalyst and CO_2 sorbent due to its low cost and abundance, and is commonly considered as the sorbent in a carbonate looping (CaL) technology. The integration of H_2 production and in-situ CO_2 capture, called sorption enhanced gasification (SEG), presents the following benefits: the heat required in endothermic gasification reactions is provided by the exothermic $CaCO_3$ formation reaction and the gasification equilibrium is favourably affected by CaO presence, leading to higher H_2 yields [19].

The concept of SEG for H_2-rich syngas production has been extensively studied and its feasibility proved for different types of biomass, including corn stalk [20,21], palm kernel shell [22], sawdust [23,24], sewage sludge [25], wood [26,27] and by-product/waste of wine production process [28]. However, only a few publications have studied the feasibility of this technology using MSW as feedstock. He et al. [29] have evaluated steam MSW SEG for H_2-rich gas production using calcined dolomite as sorbent. The effect of steam/MSW and weight hourly space velocity on gas production and composition were assessed. The experiments were carried out in a laboratory-scale fixed bed reactor at the gasification temperature of 900 °C. Their study found that the catalytic activity of dolomite was enhanced by the steam presence. At steam/MSW of 1.04, the H_2 yield and H_2 molar fraction reached the maximum, 42.98 mol H_2/kg MSW and 53.22%, respectively. Zhou et al. [30] have studied the steam MSW SEG with CaO as CO_2 sorbent in a batch-type fixed bed. They studied the impact of the gasification temperature and sorbent/ MSW ratio on the H_2 yield. They showed that the H_2 molar fraction was improved on the addition of CaO. At the gasification temperature of 700 °C and with CaO:MSW mass ratio of 1:1, the H_2 molar fraction in the syngas raised from around 35%, without sorbent, to around 50% with CaO. The CaO sorbent has also been shown to have a catalytic effect on the MSW devolatilisation and char gasification. Hu et al. [31] studied the effect of the moisture content in MSW on H_2 yield using a laboratory-scale fixed bed reactor. Their study showed that the H_2 mole fraction in the syngas achieved a maximum value of 49.4% at the gasification temperature of 750 °C, a molar ratio of CaO to carbon in MSW of 0.7 and a 40% moisture content in MSW. Irfan et al. [32] have studied the potential of using waste marble powder, whose main component is $CaCO_3$, as a catalyst and CO_2 capture sorbent in the MSW gasification. The effect of temperature, steam/MSW and sorbent/MSW on the gas composition, dry gas yield, tar content and carbon conversion efficiency were investigated in a laboratory-scale batch-type fixed bed reactor. They found the rise of the four variables analysed have a positive effect on the production of H_2-rich gas resulting in an increase in the H_2 molar fraction, the dry gas yield and the carbon conversion efficiency. On the other hand, the tar content was reduced. Martínez et al. [33] have studied the feasibility of MSW SEG for the production of synthetic fuel in a 30kW_{th} bubbling fluidised bed (BFB) pilot plant. The effect of the gasification temperature,

sorbent/MSW ratio and steam excess were also analysed. The gasification temperature was shown to have the most significant influence on the syngas composition. Importantly, for temperatures higher than 680 °C the CaO carbonation is inhibited and the amount of CO_2 captured is limited. As a result, the mole fraction of H_2 decreased and the mole fraction of CO_2 increased at temperatures above 680 °C. Their study also showed that higher contents of tar (mainly benzene and toluene) were produced than that reported in the other studies using a dual fluidised bed (DFB) [34,35]. They concluded that such enhanced tar formation could be associated with the limited low amount of sorbent present in the freeboard zone of DBF and therefore, the tar formation was promoted. However, this drawback would be overcome by a cyclic operation, where the BFB is connected to the calciner as this set-up operates at higher sorbent/MSW ratios, reducing the tar formation [33].

The feasibility assessments of SEG presented in the literature focused mainly on characterising the CO_2 capture rate and syngas composition associated with this type of gasification technology (Table 1). However, a comprehensive energy analysis, which would determine the heat required for the regeneration of CaO sorbent for the cyclic operation of MSW SEG, was not performed. Though SEG has to be shown a technically feasible option for converting MSW into valuable products, such as H_2, its commercialisation depends on the H_2 production costs. The H_2 production costs based on SEG of biomass were assessed for the first time by Schweitzer et al. [36], which reported values between 6 and 10 €/kg. However, to date no techno-economic assessment was performed for the SEG of MSW.

Therefore, this study aimed to evaluate the techno-economic feasibility of H_2 production through SEG of MSW using steam as a gasifying agent. To understand the benefits of SEG, this study benchmarked the techno-economic performance of SEG with conventional steam gasification of MSW. A parametric study was also performed to understand the impact of the steam-to-biomass ratio (SBR; both technologies) and the gasification temperature (conventional steam gasification only) on the thermodynamic performance. The impact of the economic assumptions on the economic performance was also assessed.

Table 1. Literature cases on sorption enhanced gasification of municipal solid waste

Literature Case	**This work**	**He at al.** [29]	**Zhou et al.** [30]	**Hu et al.** [31]	**Irfan et al.** [32]	**Martínez et al.** [33]
Feedstock	MSW	MSW	MSW (refused-derived fuels)	MSW	MSW	MSW-derived
Catalyst/sorbent	Limestone	Dolomite	CaO	CaO	Waste marble power	Limestone
Agent gasifying	Steam	Steam	Steam	Steam[a]	Steam	Steam
Reactor type	Dual Fluidised bed	Laboratory-scale fixed bed	Laboratory-scale batch-type fixed bed	Laboratory-scale fixed bed	Laboratory-scale batch-type fixed bed	30 kW_{th} bubbling fluidised bed
Production	H_2	Syngas	Syngas	Syngas	Syngas	Syngas
Work type	Theoretical	Experimental	Experimental	Experimental	Experimental	Experimental
Sorbent regeneration	Yes	N/A	N/A	N/A[b]	N/A	N/A
Thermodynamic analysis	Yes	N/A	N/A	N/A	N/A	N/A
Economic analysis	Yes	N/A	N/A	N/A	N/A	N/A

[a]Auto generated steam from MSW moisture

[b]Not assessed but a new cyclic process for direct gasification of wet MSW was proposed

2. Process and model description

This study benchmarked the techno-economic performance of two waste-to-fuel conversion processes, conventional steam gasification without CO_2 capture and SEG with CO_2 capture. The MSW properties were taken from Wang et al. [37], and the main properties, such as lower heating value (LHV), moisture content, ultimate and proximate analysis are presented in Table 2. The considered processes were assumed to have a processing capacity of 500 t/d of MSW, which translates to around 100 MW_{th} fuel input. The process models for the considered waste-to-fuel conversion processes were modelled in Aspen Plus®. The following assumptions were considered in both models:

- the process is steady state, isothermal with temperature and pressure uniformity;
- all the gases are ideal;
- char consists only of carbon;
- ash is inert and does not take part in any reactions; and
- tar and higher hydrocarbon formation is not considered.

The Peng-Robinson equation of state with Boston-Mathias modifications was selected to estimate the physical properties of the components. The syngas composition was determined using the minimisation of the total Gibbs free energy (*RGibbs*). The considered gasification processes usually do not achieve chemical equilibrium, leading to an overestimation of H_2 and CO production and underestimation of CO_2 and CH_4 production [38]. For this reason, the equilibrium temperatures for the WGS and methane reforming reactions were restricted. This method has previously been successfully employed to accurately represent the gasification process of different feedstocks [39].

Table 2. Ultimate and proximate analysis of municipal solid waste [37]

Properties	**Value**
LHV[1] [MJ/kg]	19.99
Moisture content [$\%_{wt}$]	9.34
Ultimate Analysis [$\%_{wt}$ db[2]]	
Elemental composition	C:49.51; H:6.42; O:35.69; N:0.78; S:0.48
Proximate Analysis [$\%_{wt}$ db[2]]	
Volatile matter	77.52
Fixed carbon	15.36
Ash	7.12

[1]lower heating value; [2]dry basis

2.1. Conventional steam gasification of municipal solid waste (Case 1)

The MSW steam gasification plant consists mainly of a gasification unit, the syngas clean-up and upgrading units, a heat exchanger network and a gas turbine. The conceptual design of the H_2 production *via* steam gasification of MSW is presented in Figure 1 and the operating conditions are summarised in Table 4.

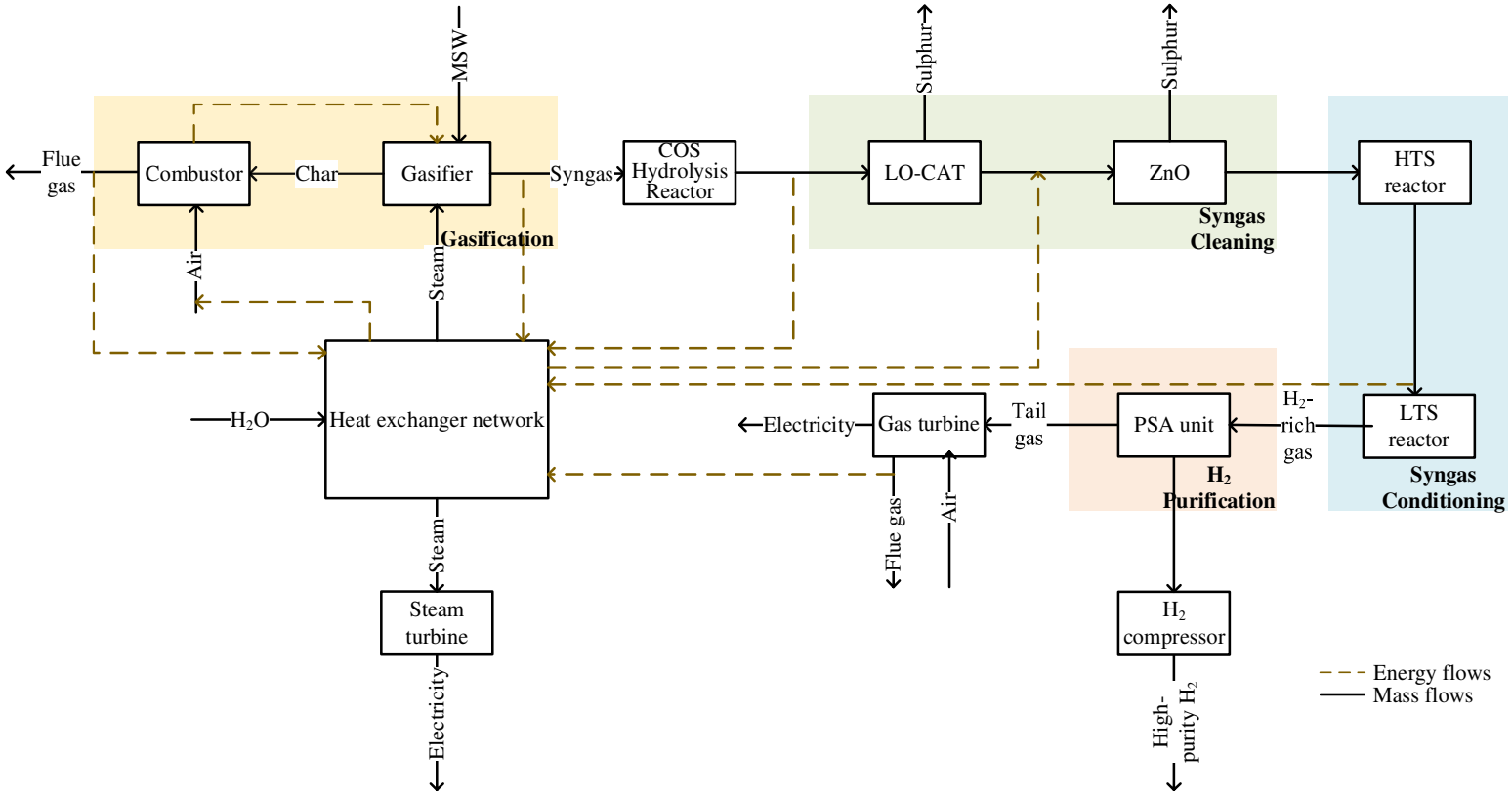

Figure 1. Simplified diagram of municipal solid waste gasification for H_2 production

Although not presented in Figure 1, it was assumed that MSW was subject to a pre-treatment before being fed to the gasifier. This is completed in two stages, a primary separation of the recyclables and a mechanical treatment to produce briquettes [40]. It is noteworthy that the power requirement of these stages was accounted for and estimated based on the data reported based on the literature data [40]. A DFB was selected as a gasifier that comprises two distinctive zones, gasification zone and combustion zone. The gasification unit was modelled using a Gibbs reactor (*RGibbs*) and a stoichiometric reactor (*RStoich*). The process model was developed based on the study by Doherty et al. [41]. In the combustor, the unconverted char is burnt in the excess amount of air (λ=1.12), providing the heat necessary to maintain a constant temperature in the gasifier. This heat is transferred to the gasifier by circulating the bed material between the two reactors. The temperature of the combustor was set to be 55 °C higher than the gasification temperature. Moreover, steam at 350 °C and 1 bar was used as the gasifying agent. The gasification process was validated with the experimental data reported by Fremaux et al. [10], considering the gas composition (Figure 2a) and H_2 yield (Figure 2b) for different temperatures (700 °C, 800 °C and 900 °C) and steam-to-biomass ratios (0.5, 0.7 and 1.0). The results presented in Figure 2 show a good agreement between the experimental results and the model predictions, indicating that the model developed in this study accurately represents the MSW steam gasification process.

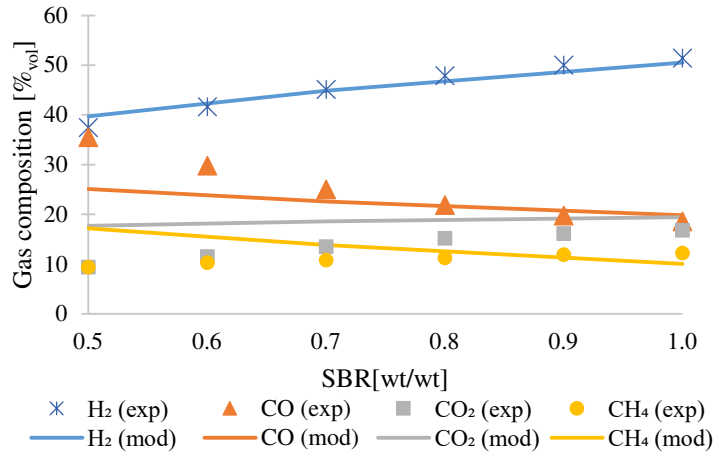

a)

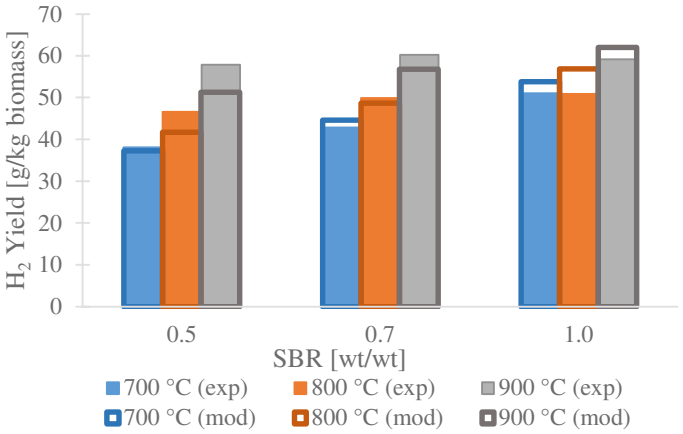

b)

Figure 2. Validation of the municipal solid waste steam gasification model with experimental data, obtained at three different temperatures and steam-to-biomass ratios, in terms of a) gas composition and b) hydrogen yield. Exp and mod correspond to experimental and simulated data, respectively. [10]

Since the activity of the reforming catalysts is negatively affected by the presence of sulphur compounds, the raw syngas leaving the gasifier is then directed to the syngas clean-up unit to reduce the H_2S concentration to around 1ppm [42]. Before the sulphur removal, the COS present in the raw syngas is converted to H_2S in the carbonyl sulphide (COS) reactor [43]. This was modelled as stoichiometric reactor (*RStoich*) with the assumption that 99.5% of COS is converted to CO_2 and H_2S. In the first stage of the syngas clean-up unit, the H_2S concentration is reduced to 11 ppm using a liquid oxidation catalyst (LO-CAT process). In a second step, a zinc oxide (ZnO) bed is used to remove the remaining sulphur to achieve the desired level of H_2S in syngas. To promote the H_2 yield, high-temperature (HTS) and low-temperature (LTS) shift reactors are employed. These reactors were modelled as equilibrium reactors (*REquil*) with the WGS reaction, Eq. (1) [44]. The performance of the WGS reactors was compared with the experimental data obtained in a pilot plant by Materazzi et al. [45]. Considering the same gas composition and operating conditions, the CO global conversion was

96.7%. Such performance is comparable with the conversion of 92.1% reported by Materazzi et al. [45]. After this stage, the H_2-rich syngas is further purified in a pressure swing adsorption (PSA) unit. It is assumed that 99.9% H_2 purity can be achieved with a H_2 recovery rate of 85% [42]. Although this unit is not modelled in detail in this study, its energy requirement and associated costs were accounted for. The H_2 stream is then compressed to 60 bar and the tail gas is routed to the gas turbine where is burnt in the combustor. The flue gas is then mixed with bleed compressed air to reduce the turbine inlet temperature below 1250 °C. The heated and compressed gas is then expanded in the turbine generating mechanical work required to generate electricity. Additionally, a heat exchanger network and steam cycle are also considered for heat recovery and electricity production. The considered steam cycle is based on a superheated Rankine cycle, which has already been validated and described in detail in Santos et al. [46].

2.2. Sorption enhanced gasification of municipal solid waste (Case 2)

Similarly to the conventional steam gasification considered in Case 1, SEG also uses the dual fluidised bed layout. However, the material circulated between the interconnected fluidised beds acts simultaneously as the heat and CO_2 carrier. Since the CO_2 is removed by the sorbent in the sorption enhanced gasifier, the equilibrium of the WGS, Eq. (1), shifts to the right, leading to an enhanced H_2 yield. A simplified diagram of the MSW SEG plant is depicted in Figure 3. As can be seen, the WGS reactors and the syngas clean-up unit (LO-CAT and ZnO beds) are not present in the SEG process. This is because these are replaced by the sorption enhanced gasifier where the CO_2 capture also takes place. The calciner, PSA unit, CO_2 compression unit, heat exchanger network and gas turbine are the remaining main components of the SEG process. Similarly to conventional steam gasification, it was assumed that a pre-treatment comprising primary separation and mechanical treatment is required to obtain a feedstock suitable for gasification. Therefore, the power requirement of this treatment was also taken into account.

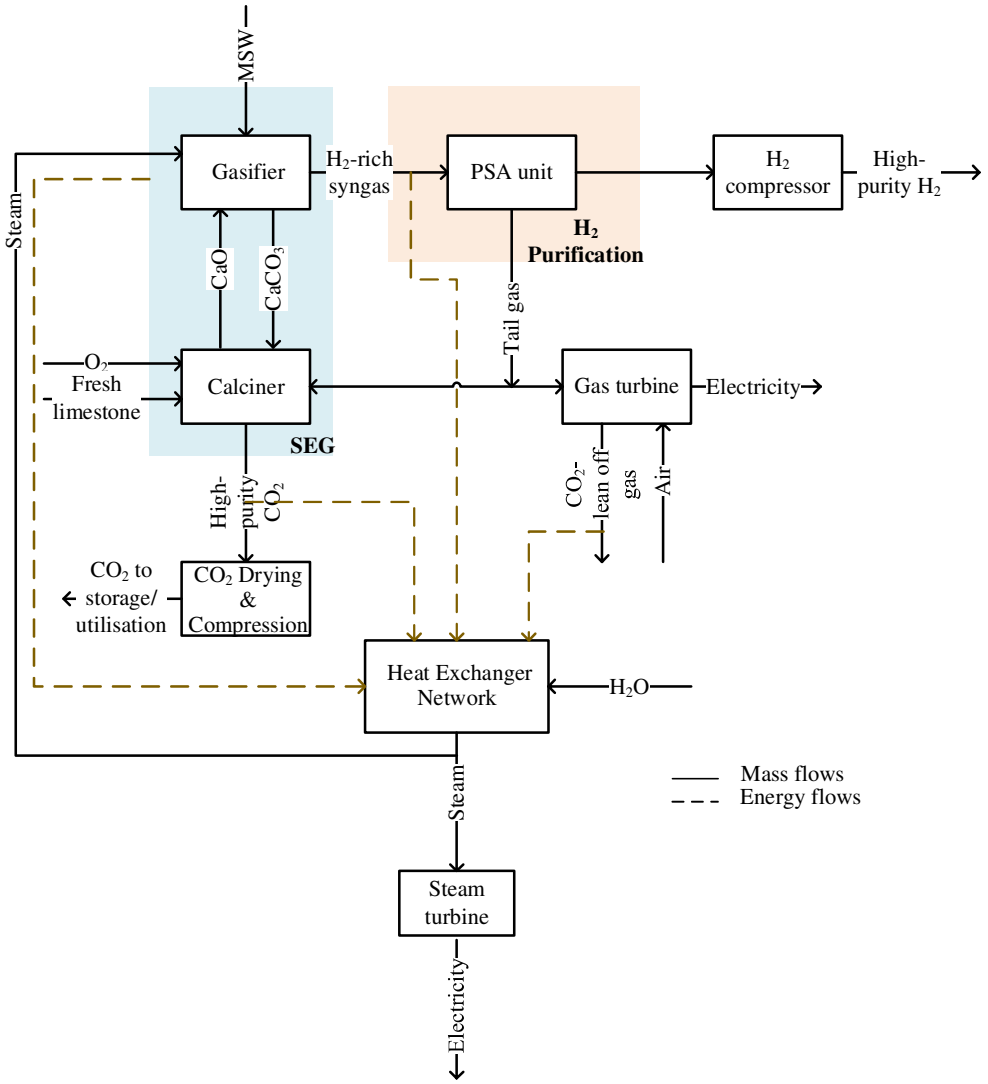

Figure 3. Simplified diagram of municipal solid waste sorption enhanced gasification for hydrogen production

To model the sorption enhanced gasifier in Aspen Plus®, two reactors (a Gibbs reactor and a stoichiometric reactor) are connected with a heat stream. The raw syngas produced during the steam gasification (steam at 350 °C and 1 bar), which occurs in the first reactor, is directed to the second reactor where the CO_2 produced during the gasification is captured by the CaO, Eq. (2). As a result, the energy demand for the gasification reaction is met by the sensible heat carried by the sorbent and the heat released during the carbonation reaction. The WGS reaction occurs simultaneously during the CO_2 capture process, leading to the production of H_2-rich syngas. The decomposition of $CaCO_3$, formed in the sorption enhanced gasifier, into CaO and CO_2 occurs in the calciner, Eq. (3). Because the calcination reaction is endothermic, the unconverted char transported from the sorption enhanced gasifier and part of the tail gas from the PSA unit are combusted directly in the calciner. To achieve a high-purity CO_2 stream, pure O_2 is used for combustion in the calciner. The O_2 is produced in a cryogenic air separation unit (ASU), the energy requirement of which was assumed to be 200 $kW_{el}h/tO_2$ [47]. The high-purity

stream of CO_2 is then cooled to 25°C and compressed to 110 bar [48]. The H_2-rich stream is fed to the PSA unit where H_2 is separated from other gaseous impurities. Because SEG includes both gasification and CO_2 capture, the composition of H_2-rich syngas is different (H_2:79.9%$_{vol}$; CO:5.6%$_{vol}$; CO_2:2.7%$_{vol}$; CH_4:11.1%$_{vol}$) than that received in the conventional steam gasification (H_2:68.7%$_{vol}$; CO:0.1%$_{vol}$; CO_2:29%$_{vol}$; CH_4:1.6%$_{vol}$) processes. Therefore, it was assumed that a high-purity H_2 stream (99.9%) is produced with an H_2 recovery rate of 93% [49,50]. The tail gas from the PSA unit is used as fuel in the process. A part of the tail gas is used in the calciner, providing heat for calcination, whereas the remaining amount is used in a gas turbine to produce electricity. A heat exchanger network is also considered to recover the high-grade heat of H_2-rich syngas, CO_2-lean off gas and high-purity CO_2 streams that, along with the heat from SEG, are used for steam production. The approach to gas turbine and steam cycle modelling was described in detail in the previous section. The main input parameters and operating conditions for SEG are described in Table 4.

Water Gas Shift: $CO(g) + H_2O(g) \rightarrow CO_2(g) + H_2(g)$	$\Delta H = \pm 40.9$ kJ/mol	(1)
Carbonation: $CaO(s) + CO_2(g) \rightarrow CaCO_3(s)$	$\Delta H = -178$ kJ/mol	(2)
Calcination: $CaCO_3(s) \rightarrow CaO(s) + CO_2(g)$	$\Delta H = 178$ kJ/mol	(3)

The developed SEG model was validated as two separated processes, the steam gasification process described in the previous section (Figure 2) and calcium looping (CaL). The experimental results obtained at a 20 kW_{th} dual fluidised bed by Armbrust et al. [51] were used to validate the CaL process. The simulated results were compared with the experimental data obtained at different operating conditions, such as syngas composition, carbonator temperature and looping ratio (molCa/(molCO+molCO$_2$)). The operating conditions of each run are presented in Table 3. This comparison, depicted in Figure 4, shows that the model can well describe the experimental results.

Table 3. Operating conditions of each run used to validate the calcium looping model [51]

Run	Parameter	Value
1	Syngas mole fraction [%$_{vol,dry}$]	H_2:51.4; CO:20.9; CO_2:23.4; CH_4+C_xH_y: 4.3
	Carbonator temperature [°C]	637
	Looping ratio	7
2	Syngas mole fraction [%$_{vol,dry}$]	H_2:55.9; CO:12.9; CO_2:23.2; CH_4+C_xH_y:8.0
	Carbonator temperature [°C]	643
	Looping ratio	8.6

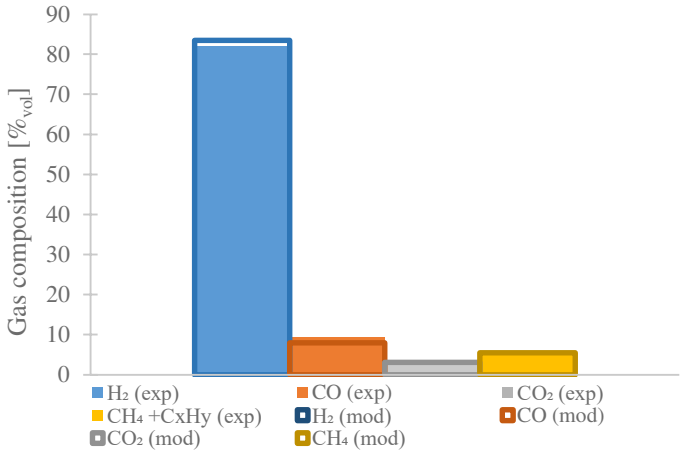

a)

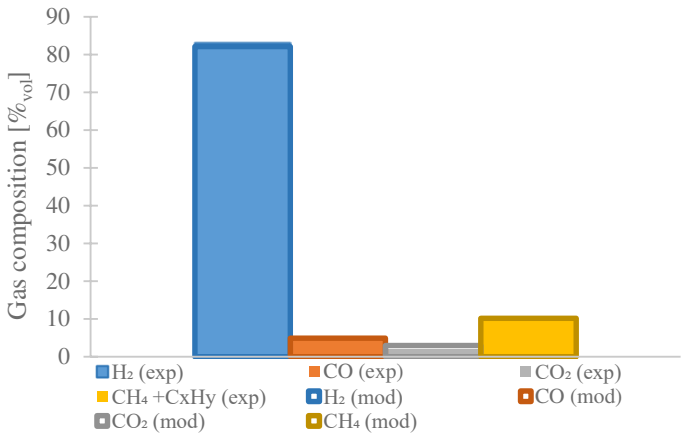

b)

Figure 4. Sorption enhanced gasification validation with literature data for different operating conditions: a) Run 1 and b) Run 2 presented in Table 3. Exp and mod correspond to experimental and simulated data, respectively. [51]

Table 4. Main model assumptions used for gasification and sorption enhanced gasification

Unit operation	Parameter	Value
Gasification	Temperature [°C]	650-1000
	Pressure [bar]	1
	Gasifier type	Dual fluidised bed
	Steam-to-biomass ratio [wt/wt]	0.5-1.3
Syngas clean-up		
COS hydrolysis	Temperature [°C]	200
LO-CAT	Temperature [°C]	50
	Outlet H_2S [ppm]	11
ZnO	Temperature [°C]	375
	Outlet H_2S [ppm]	1
Syngas upgrading		
HTS	Temperature [°C]	350
LTS	Temperature [°C]	200
PSA	H_2 recovery [%]	85.0
	H_2 purity [$\%_{vol}$]	99.9
	Temperature [°C]	30
	Feed pressure [bar]	25
	Tail gas pressure [bar]	1
	Delivery pressure [bar]	60
Sorption enhanced gasification		
Sorption enhanced gasifier	Temperature [°C]	650
	Steam-to-biomass ratio [mass basis]	0.5-2
	Carbonated sorbent fraction [-]	0.7
	CO_2 capture efficiency in carbonator [%]	90.0
Calciner	Temperature [°C]	900
	Calcined sorbent fraction [-]	0.95
	Excess oxygen [$\%_{vol,dry}$]	2.5
	Relative make-up [-]	0.02
H_2-rich syngas upgrading		
PSA	H_2 recovery [%]	93.0
	H_2 purity [$\%_{vol}$]	99.9
	Temperature [°C]	30
	Feed pressure [bar]	34
	Tail gas pressure [bar]	1
	Delivery pressure [bar]	60
CO_2 compression		
Compressors	Polytropic efficiency [%]	80.0
	Mechanical efficiency [%]	99.6
Pump	Isentropic efficiency [%]	80.0
	Mechanical efficiency [%]	99.6
CO_2 final stream	Temperature [°C]	25.0
	Pressure [bar]	110.0
Steam Cycle		
Live Steam	Temperature [°C]	593.0
	Pressure [bar]	154.0
High-pressure turbine	Isentropic efficiency [%]	92.0
	Mechanical efficiency [%]	99.8
Intermediate-pressure turbine	Isentropic efficiency [%]	94
	Mechanical efficiency [%]	99.8
Low-pressure turbine	Isentropic efficiency [%]	88
	Mechanical efficiency [%]	98
Condenser	Feed water temperature [°C]	10.0
Gas turbine	Compressor outlet pressure [bar]	20
	Combustor pressure drop [%]	2
	Turbine inlet temperature [°C]	1268
	Turbine isentropic efficiency [%]	80
	Turbine mechanical efficiency [%]	99.6
Fresh material [52]	Limestone (95.0%$_{wt}$ $CaCO_3$, 3.5%$_{wt}$ $MgCO_3$, 0.6%$_{wt}$ SiO_2, 0.4%$_{wt}$ Fe_2O_3, 0.5%$_{wt}$ Al_2O_3)	

3. Techno-economic feasibility assessment

To understand the benefits of SEG, the process models described in Section 2 were used to assess the techno-economic performance of conventional steam gasification and SEG.

3.1. Thermodynamic performance indicators

Four parameters were used to assess and compare the thermodynamic performance of the considered cases, including H_2 production efficiency, gross power efficiency, net power efficiency and total efficiency were the indicators selected for comparison. The H_2 production efficiency (η_{H_2}), Eq. (4), is defined as the ratio of the H_2 chemical energy and the chemical energy of MSW. It is noteworthy that all the indicators are calculated based on the lower heating value of H_2 (LHV_{H_2}) and MSW (LHV_{MSW}). In Eq. (4), $\dot{m}_{H_2}$ and $\dot{m}_{MSW}$ are the H_2 and MSW mass flowrates, respectively.

$$\eta_{H_2} = \frac{\dot{m}_{H_2} \cdot LHV_{H_2}}{\dot{m}_{MSW} \cdot LHV_{MSW}} \tag{4}$$

The gross power efficiency ($\eta_{el,gross}$), given by Eq. (5), is defined as the ratio of the gross electric power output ($W_{el,gross}$) and the chemical energy of MSW. The former accounts the electricity generated in the steam cycle and the gas turbine.

$$\eta_{el,gross} = \frac{W_{el,gross}}{\dot{m}_{MSW} \cdot LHV_{MSW}} \tag{5}$$

The ratio between the net electric power output and the total chemical energy of MSW, calculated by Eq. (6), defines the net power efficiency ($\eta_{el,net}$). The net electric power output ($W_{el,net}$) is the gross electric power output minus the electric power required to run the auxiliary equipment.

$$\eta_{el,net} = \frac{W_{el,net}}{\dot{m}_{MSW} \cdot LHV_{MSW}} \tag{6}$$

Finally, the total efficiency η_{tot}, defined in Eq. (7), is the sum of H_2 production efficiency and the net power efficiency.

$$\eta_{tot} = \frac{\left(\dot{m}_{H_2} \cdot LHV_{H_2}\right) + W_{el,net}}{\dot{m}_{MSW} \cdot LHV_{MSW}} \tag{7}$$

3.2. Economic performance indicators

The economic performance of the considered cases was assessed in terms of the levelised cost of hydrogen (*LCOH*), and the cost of CO_2 avoided (*AC*). The levelised cost corresponds to the minimum hydrogen sale price at which the net present value (*NPV*), given by Eq. (8), reaches zero.

$$NPV = \sum_{t=1}^{n} \frac{CF_t}{(1+r)^t} - TCR \tag{8}$$

The NPV method estimates the discounted cash flow (CF_t) throughout the project lifetime (t), accounting for the total capital requirement (TCR), which was estimated following the approach described in Table 5, and the project discount rate (r). Since the inflation was not considered, the material and feedstock prices considered in the beginning of the project were valid for the project lifetime. These costs and other economic parameters are presented in Table 6. The cost correlations used on the estimation of capital cost of each unit are shown in Table 7. For the conventional steam gasification case, the annual operating and maintenance costs, the sum of variable and fixed costs, were calculated assuming a fraction of the TCR. It was assumed 6.6% of TCR to cover the variable operating costs (raw materials and utilities) and 6.7% of TCR to account the fixed costs [42]. In the SEG case, the variable costs account the costs of raw materials, utilities along with the cost associated with CO_2 transport and storage. Since the economic assessment of this technology is very scarce in the literature, the fixed costs were estimated based on the figures reported by Schweitzer et al. [36]. It was assumed that 10%, 4%, 2% and 1.8% of TCR covered the costs relating to the working capital, maintenance (labour & material), insurances & taxes and the plant overhead costs, respectively.

Table 5. Economic approach used for total capital requirement estimation [53]**.**

	Correlation [€]
Actual capital cost of j-component (C_j)	$C_j = C_{j,0}\left(\frac{CEPCI_{2017}}{CEPCI_0}\right)$
Total installed cost *(TIC)*	$TIC = \sum C_j$
Engineering procurement and construction *(EPC)*	$EPC = 10\%TIC$
Contingency plan *(PC)*	$PC = 20\%(TIC+EPC)$
Total plant cost *(TPC)*	$TPC = TIC+EPC+PC$
Other capital costs *(OCAPEX)*	$OCAPEX = 20\%TPC$
Total capital requirement *(TCR)*	$TCR = 18\%(TPC+OCAPEX)$

Table 6. Main economic parameters and assumptions.

Parameter	**Value**
Unit cost of electricity exported to the grid [€/$MW_{el}h$] [54]	40.0
Limestone unit cost [€/t] [36]	11.6
Clean water unit cost [€/m^3] [36]	2.4
CO_2 transport and storage cost [€/t] [55]	20.0
Others	
Expected lifetime [y] [56,57]	25.0
Project interest rate [%] [56,57]	8.8
Capacity factor [%] [56,57]	80.0
Average USD/EUR exchange rate 2017 [58]	0.8898
Average GBP/EUR exchange rate 2017 [58]	1.1418
CO_2 emission allowance price [€/tCO_2] [59]	39.6
Gate fee [€/t_{MSW}] [60]	40.0

The cost CO_2 avoided (AC), represented by Eq. (9), is calculated based on the LCOH and the CO_2 emission intensity determined for both plants.

$$AC = \frac{LCOH_{SEG} - LCOH_{Gasf}}{e_{CO_2,eq,Gasf} - e_{CO_2,eq,SEG}} \quad (9)$$

The CO_2 emission intensity accounts the direct $\left(\boldsymbol{e_{CO_2}}\right)$ and indirect $\left(\boldsymbol{P_e \cdot e_{CO_2,e}}\right)$ CO_2 emissions, which is defined by the equivalent CO_2 emissions ($\boldsymbol{e_{CO_2,eq}}$), Eq. (10). The indirect emissions are associated with the surplus or deficit of electricity generated ($\boldsymbol{P_e}$) and therefore, depend on the power plant characteristics. In that case, it was assumed the power plant emits 262 $\mathbf{kg_{CO_2}}$ per 1 $MW_{el}h$ of electricity generated with an efficiency of 45.9 %, which were determined take into account the power generation of the 27 EU Member States and UK in 2015 [61].

$$e_{CO_2,eq} = e_{CO_2} + Pe \cdot e_{CO_2,e} \quad (10)$$

Table 7. List of cost correlations used on the estimation of capital cost of each unit (C_j).

Unit operation	Cost Correlation
Gasifier [Inlet steam flowrate, $\dot{m}_{Steam}$(kg/h)] [62]	$C_{Gasf} = 6.5e6 \left(\frac{\dot{m}_{Steam}}{226.8}\right)^{0.6}$
LO-CAT oxidiser vessel [Sulphur removed flowrate, $\dot{m}_S$ (kg/h)] [42]	$C_{LO\text{-}CAT} = 1.0e6 \left(\frac{\dot{m}_S}{234.5}\right)^{0.65}$
ZnO bed [Inlet syngas flowrate, $\dot{m}_{Syngas}$(kg/h)] [42]	$C_{ZnO} = 3.7e4 \left(\frac{\dot{m}_{Syngas}}{81371.7}\right)^{0.56}$
HTS reactor [Inlet syngas flowrate, $\dot{m}_{Syngas}$ (kg/h)] [42]	$C_{HTS} = 4.65907e5 \left(\frac{\dot{m}_{Syngas}}{160763.9}\right)^{0.56}$
LTS reactor [Inlet syngas flowrate, $\dot{m}_{Syngas}$ (kg/h)] [42]	$C_{LTS} = 3.23464e5 \left(\frac{\dot{m}_{Syngas}}{160763.9}\right)^{0.56}$
Pressure swing adsorption unit [Inlet gas molar flowrate, $\dot{n}_{PSA}$ (kmol/h)] [63]	$C_{PSA} = 27.96e6 \left(\frac{\dot{n}_{PSA}}{17069}\right)^{0.60}$
H_2 compressor [Brake power requirement, $\dot{W}_{H_2,BRK}$ (kW_{el})] [63]	$C_{H_2Comp} = 1200 \left(\frac{\dot{W}_{H_2,BRK}}{0.746}\right)^{0.82}$
Sorption enhanced gasifier [Installed capacity LHV, P_{inst} (MW)] [36]	$C_{SEG} = 22.1e6 \left(\frac{P_{inst}}{10}\right)^{0.80}$
Calciner [Calciner heat flux, $\dot{Q}_{calc}$ (kW_{th})] [64]	$C_{calc} = 13140\ (\dot{Q}_{cal})^{0.67}$
Air separation unit [O_2 production rate, $\dot{m}_{O_2}$(kg/s)] [65]	$C_{ASU} = 2.926e7 \left(\frac{\dot{m}_{O_2}}{28.9}\right)^{0.70}$
CO_2 compression unit [Brake power requirement, $\dot{W}_{CCU,BRK}$ (kW_{el})] [66]	$C_{CCU} = 1.22914e7 \left(\frac{\dot{W}_{CCU,BRK}}{13000}\right)^{0.67}$
Gas turbine [Inlet air flowrate, $\dot{m}_{Air}$ (kg/s)] [63]	$C_{GT} = 31.5e6 \left(\frac{\dot{m}_{Air}}{209}\right)^{0.85}$
Fuel compressor [Brake power requirement, $\dot{W}_{FC,BRK}$ (kW_{el})] [67,68]	$C_{FC} = 91562 \left(\frac{\dot{W}_{FC,BRK}}{445}\right)^{0.67}$
Steam Cycle	
High-pressure steam turbine [Brake power output, $\dot{W}_{HPST,BRK}$ (kW_{el})] [69]	$C_{HPST} = 33.7e6 \left(\frac{\dot{W}_{HPST,BRK}}{200000}\right)^{0.67}$
Intermediate-pressure steam turbine [Brake power output, $\dot{W}_{IPST,BRK}$ (kW_{el})] [69]	$C_{IPST} = 33.7e6 \left(\frac{\dot{W}_{IPST,BRK}}{200000}\right)^{0.67}$
Low-pressure steam turbine [Brake power output, $\dot{W}_{LPST,BRK}$ (kW_{el})] [69]	$C_{LPST} = 33.7e6 \left(\frac{\dot{W}_{LPST,BRK}}{200000}\right)^{0.67}$
Deaerator [Inlet flowrate, $\dot{m}_{DEA}$ (kg/h)] [42]	$C_{DEA} = 1.30721e5 \left(\frac{\dot{m}_{DEA}}{157970.7}\right)^{0.72}$
Deaerator feed pump [Condensate flowrate, $\dot{m}_{COND}$ (kg/h)] [42]	$C_{P\_DEA} = 8679 \left(\frac{\dot{m}_{COND}}{158425.2}\right)^{0.33}$
Low-pressure water pump [Feed water flowrate, $\dot{m}_{LPW}$ (kg/h)] [42]	$C_{P\_LPW} = 95660 \left(\frac{\dot{m}_{LPW}}{158425.2}\right)^{0.33}$
Fresh water pump [Fresh water flowrate, $\dot{m}_{CW}$ (kg/h)] [42]	$C_{P\_CW} = 5437 \left(\frac{\dot{m}_{CW}}{42625.9}\right)^{0.33}$
Heat exchanger GT flue gas cooler/Steam generator [PINCH, $\dot{Q}_{GT-SG}$ (kW_{th})] [42]	$C_{GT\text{-}SG} = 26143 \left(\frac{\dot{Q}_{GT-SG}}{401.5}\right)^{0.60}$
Heat exchanger Syngas cooler/Steam generator [PINCH, $\dot{Q}_{Syngas-SG}$ (kW_{th})] [42]	$C_{Syngas\text{-}SG} = 26143 \left(\frac{\dot{Q}_{Syngas-SG}}{401.5}\right)^{0.60}$
Condenser [Heat exchange area, A_{COND} (m^2)] [70]	$C_{COND} = 8500 + 490(A_{COND})^{0.85}$
Heat exchanger live steam [Heat exchange area, A_{LS} (m^2)] [68]	$C_{LS} = 2290(A_{LS})^{0.60}$
Heat exchanger condensate [Heat exchange area, A_{COND} (m^2)] [67]	$C_{COND} = 130 \left(\frac{A_{COND}}{0.093}\right)$
Heat recovery steam generator [Steam flowrate, Q_{HRSG} (kg/h)] [43]	$C_{HRSG} = 42427 \left(\frac{AQ_{HRSG}}{277458}\right)^{0.7}$
Air preheater [Heat exchange area, A_{AXPH} (m^2)] [67]	$C_{OXPH} = 130 \left(\frac{A_{AXPH}}{0.093}\right)$
Syngas preheater [Heat exchange area, $AS_{yngasPH}$ (m^2)] [67]	$C_{OXPH} = 130 \left(\frac{A_{SyngasPH}}{0.093}\right)$
Heat exchanger high-pressure water [Heat exchange area, A_{HPW} (m^2)] [67]	$C_{HPW} = 130 \left(\frac{A_{HPW}}{0.093}\right)$
Economiser [Heat exchange area, A_{ECON} (m^2)] [67]	$C_{ECON} = 130 \left(\frac{A_{ECON}}{0.093}\right)$
Pre-treatment [Processing capacity, $\dot{m}_{MSW}$(t/h)] [40]	$C_{Pre\text{-}t} = (9.0e4\dot{m}_{MSW} + 6.6e4) + (7.1e4\dot{m}_{MSW} + 8.0e4)$

4. Results and discussion

The parameters and design specifications presented in Section 3 were used to evaluate the techno-economic feasibility of SEG, which was benchmarked with the techno-economic performance of conventional steam gasification. A sensitivity analysis was also carried out to study the impact of the main economic parameters on the cost of CO_2 avoided.

4.1. Thermodynamic performance

To set the baseline for techno-economic assessment, the performance of the conventional steam gasification was first assessed.

4.1.1. Conventional steam gasification

First, the effect of the gasification temperature on the H_2 yield and on the overall system performance was investigated by varying the gasification temperature between 650 °C and 1000 °C under constant SBR of 1.0. It can be seen from Figure 5 that H_2 yield increased from 60 g/kg dry MSW to 78.8 g/kg dry MSW with the temperature rise from 650 °C, to 900 °C, at which the H_2 production reached the maximum. At higher temperatures, a slightly decrease in H_2 yield was observed. This can be attributed to the reverse WGS reaction that shifts the equilibrium and favours the reactants, consuming the H_2 and CO_2 [71]. As expected, the temperature increase favours the endothermic reaction, steam-methane reforming, enhancing the H_2 and CO formation and the CH_4 consumption. The increase of the temperature from 600 °C to 1000 °C resulted in a reduction of the gross power output from 36.4 MW to 19.4 MW. However, the net power output remained almost constant (between 6 MW and 7 MW). This can be explained by the reduced amount of the tail gas available from PSA at higher gasification temperatures, resulting in a reduced electricity production in the gas turbine, but also reduced compression energy requirement. It should be noted the energy requirement for MSW pre-treatment was accounted for and was assumed to be constant since the MSW flowrate was kept constant in all considered cases [40]. While the H_2 production efficiency (47.3%) reached the maximum at 900 °C, the net power efficiency had varied slightly, changing between 6.8% at 650 °C and 7.0% at 1000 °C. On the contrary, the gross power efficiency decreased from 34.7% to 18.5% within the same temperature range. Although the maximum total efficiency (53.0%) was obtained at 950 °C, further assessment will consider the gasification temperature of 900 °C as it maximises the efficiency of H_2 production that is the main product of the considered cases.

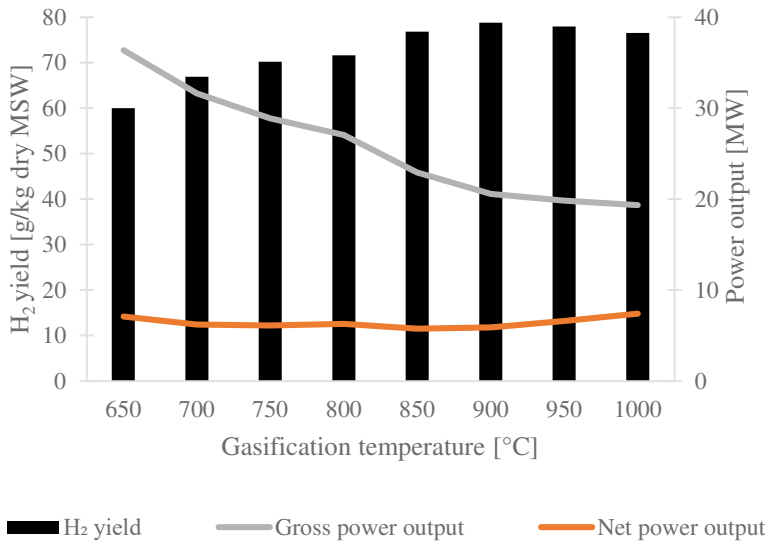

a)

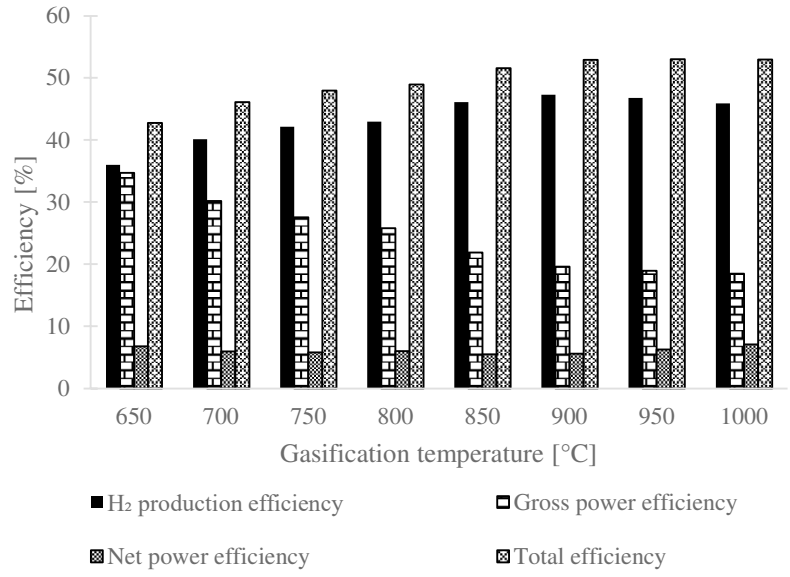

b)

Figure 5. Effect of gasification temperature on (a) hydrogen yield, gross and net power outputs, and (b) hydrogen production, gross power, net power and total efficiencies for conventional steam gasification at steam-to-biomass ratio of 1.0.

The influence of SBR on the H_2 yield and the thermodynamic performance was assessed by varying the SBR between 0.5 and 1.3 at 900 °C. Figure 6 revealed that an increase in SBR led to an increase in the H_2 yield. However, the effect of SBR on H_2 yield was observed to be less pronounced than that of the gasification temperature. This behaviour is in agreement with the experimental results reported by Rapagnà et al. [72]. The effect of SBR can be explained by the enhancement of the WGS and steam-methane reforming reactions that shift the equilibrium to the right, enhancing the H_2 formation. The increase of the SBR from 1.1 to 1.3 caused a marginal increase (0.4%) in the H_2 yield,

from 79.3 g/kg dry MSW to 79.6 g/kg dry MSW. This corresponded to a H_2 production efficiency between 47.6% and 47.8%, respectively. In the considered SBR range, the gross power output decreased from 26.0 MW to 19.6 MW and the net power output increased from 6.0 MW to 6.6 MW. Therefore, the gross power efficiency decreased from 24.8% to 18.7% and the net power efficiency increased slightly from 5.7% to 6.3%. The maximum total efficiency obtained was 54.0% at the SBR of 1.3. As can be seen in Figure 6, the difference between the two last points (SBR of 1.2 and 1.3), for all the considered indicators, was less than 1%. Therefore, it was concluded that the SBR of 1.2 resulted in the optimal operating conditions for the conventional steam gasification.

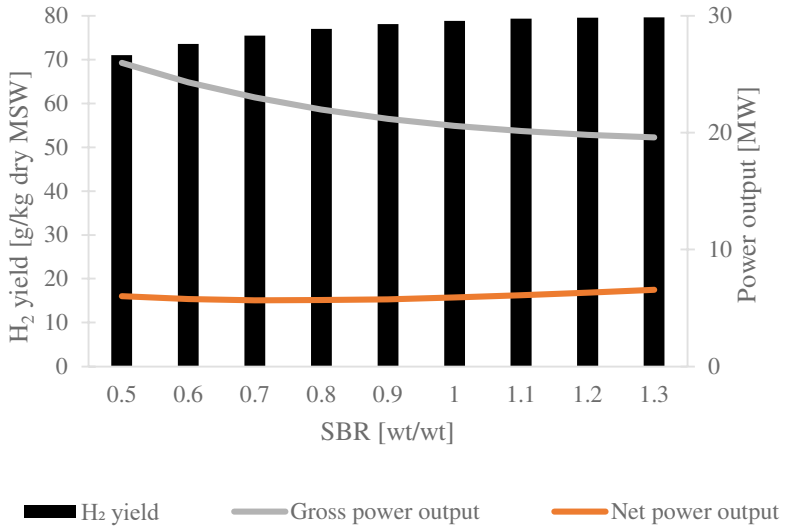

a)

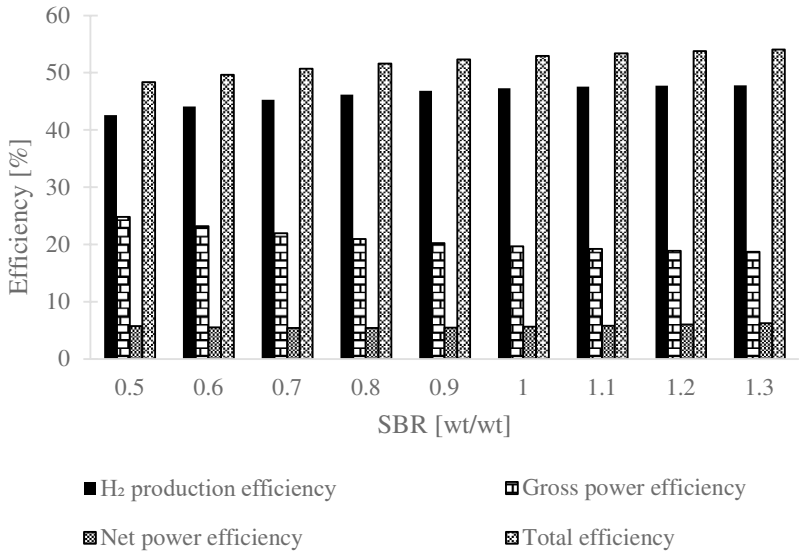

b)

Figure 6. Effect of steam-to-biomass ratio on (a) hydrogen yield, gross and net power outputs, and (b) hydrogen production, gross power, net power and total efficiencies for conventional steam gasification at gasification temperature of 900 °C

4.1.2.Sorption enhanced gasification

Similarly to the conventional steam gasification, a parametric analysis was performed to evaluate the effect of SEG operating conditions on the H_2 yield and the thermodynamic performance. However, in case of SEG, the gasification temperature was assumed to be 650 °C. This was because the carbonation reaction becomes the limiting factor at temperatures higher than 680 °C [33]. Moreover, Armbrust et al. [51] studied three carbonator temperatures (606 °C, 637 °C and 697 °C) in CaL for H_2 production from syngas and concluded that the maximum CO conversion and CO_2 capture rate were achieved at 637 °C. Although the SEG temperature was fixed at 650 °C in this study, the SBR was varied from 0.5 to 2, which corresponded to a molar steam-to-carbon (S/C) of 0.6–2.4. Figure 7 presents the effect of the SBR on the thermodynamic performance of SEG. It can be observed that the H_2 yield increased gradually on an increase in the SBR, while the gross and net power output reduced. This can be explained by the fact that less tail gas from the PSA was available to be burnt in the gas turbine, more energy was required for steam production and CO_2 compression, and less heat excess was available for power generation by the steam cycle. Thus, the maximum H_2 production efficiency maximum (51.2%) was achieved at SBR of 2.0. However, at such SBR, the gross and net efficiencies were 13.6% and -1.2%, respectively. The negative value for the net efficiency means that the available power output of the system was insufficient to meet its power requirement. Therefore, further assessment of SEG assumes the SBR of 1.8, as at this SBR the SEG process self-sufficient and there is no need to use electricity from the grid to support its operation (Figure 7b).

Comparing the considered gasification technologies, the H_2 production efficiency is almost 4% points higher for the SEG than the optimum value obtained for conventional steam gasification (47.3%). However, a trade-off between H_2 yield and power efficiency should also be considered. For the optimal operating conditions of SEG (SBR=1.8; S/C=2.2), a H_2 production efficiency of 48.7% and a total efficiency of 49.3% were obtained. Yet, the latter was lower than that obtained for conventional steam gasification (53.7%). This can be attributed to the higher power demand by SEG which translated into a net power efficiency of 0.6% that is around 5% points lower than the figure obtained for conventional steam gasification. The H_2 production efficiency is comparable with the SEG performance obtained by Detchusananard et al.[26], who reported the H_2 production efficiency of around 56% for a sorption enhanced chemical looping process operating with a S/C of 3.0.

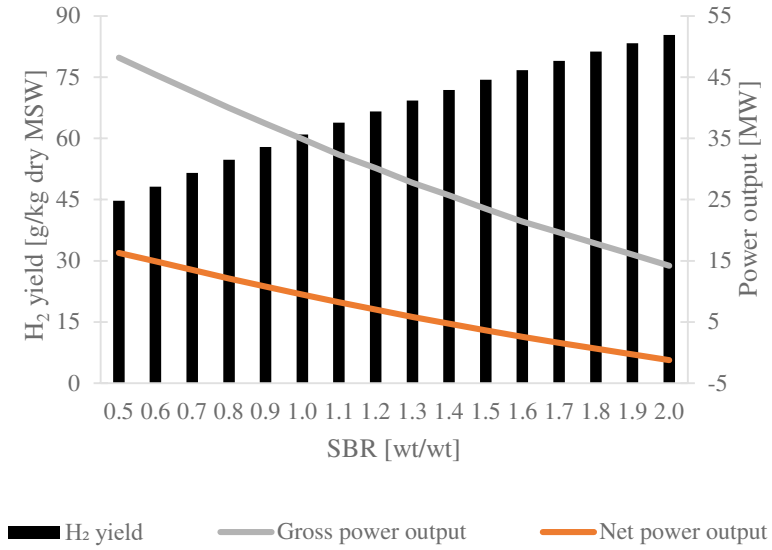

a)

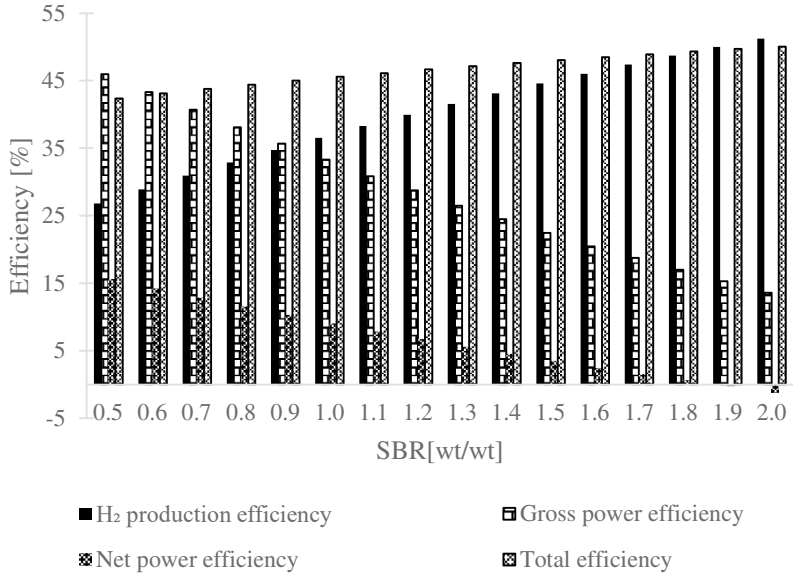

b)

Figure 7. Effect of steam-to-biomass ratio on (a) hydrogen yield, gross and net power outputs, and (b) hydrogen production, gross power, net power and total efficiencies for sorption enhanced gasification at gasification temperature of 650 °C.

4.2. Economic performance

The breakdown of total capital costs for the conventional steam gasification and SEG are shown in Figure 8. It can be observed that the gasification units in both cases were the most expensive pieces of equipment, accounting for 71% and 77% of the total capital cost, respectively. It should also be noted that the data to estimate the cost of SEG is scarce in the current literature. For this reason, the capital

cost estimate of the SEG bears significant uncertainty and is subject to sensitivity analysis later in this study. For the remaining costs, the heat network (12%) and H_2 purification and upgrading (9%) accounted for 21% of the total capital cost of the conventional steam gasification unit. For SEG, these units accounted for 10% of the total capital, with a share of 5% of each. This was due to the higher share of SEG unit and the additional units required for SEG. These units, ASU (5%) and CO_2 compression unit (4%), accounted for 9% of the total capital cost of SEG.

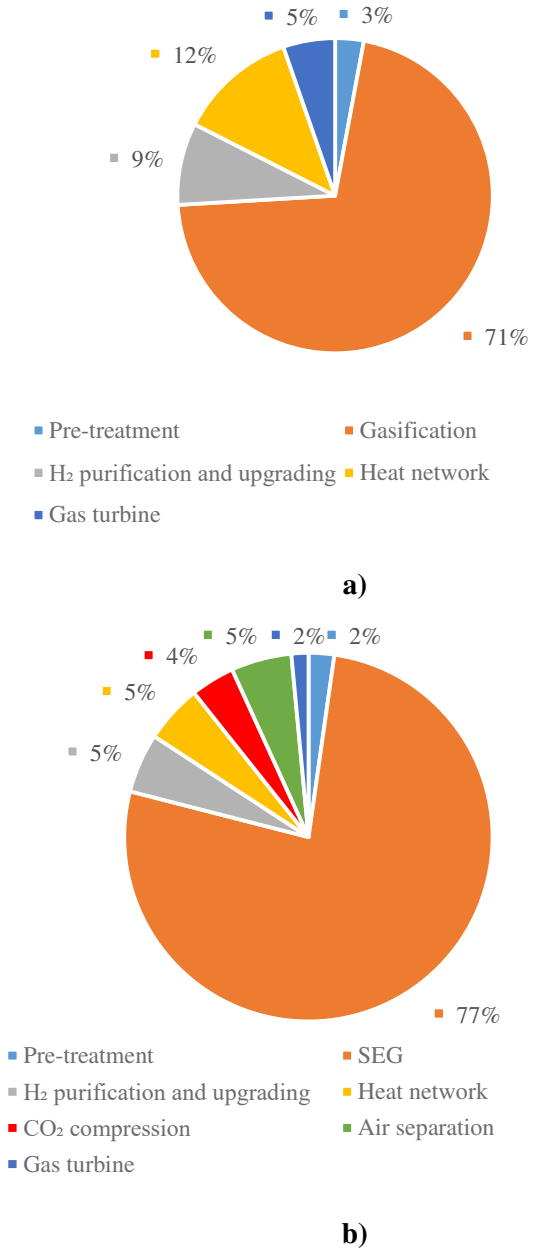

Figure 8. Split of total capital costs for (a): gasification and (b): sorption enhanced gasification

As there is still a high degree of uncertainty associated with the carbon capture and storage (CCS) technologies and the CO_2 allowances, the economic indicators considered in this study were evaluated under different scenarios.

Scenario 1: No gate fee and no fossil CO_2 emissions tax (baseline scenario)

Scenario 2: Gate fee and no fossil CO_2 emissions tax

Scenario 3: No gate fee and fossil CO_2 emissions tax

Scenario 4: Gate fee and fossil CO_2 emissions tax

A gate fee, which is a tax levied by the waste management facility, of 40.0 €/t_{MSW} was assumed [60]. Although the MSW composition may vary depending on the location or the time of the year, it was assumed that 40% of the carbon present in the MSW was of biogenic origin [60]. It should be noted that the CO_2 released during the calcination of fresh limestone make-up in SEG is of fossil origin [46]. This was accounted for in the economic assessment of Scenario 3 and Scenario 4. Under the current EU Emissions Trading System (ETS), the biogenic CO_2 emissions are considered carbon neutral. Therefore, only the CO_2 emissions of fossil origin are subject to the CO_2 emission allowance (EUA) price. The EUA price has been increasing since the end of 2020, reaching 50.0 €/tCO_2 for the first time in 2021. Therefore, an average value for the first 3 months of 2021 was taken, 39.6 €/tCO_2 [59].

Figure 9 presents the LCOH, which was estimated for both considered gasification technologies, and the cost of CO_2 avoided estimated under different scenarios. The economic evaluation showed that consideration of the CO_2 capture in SEG increased the LCOH. While for conventional steam gasification the LCOH varied between 2.1 and 3.2 €/kg, for SEG the LCOH almost doubled (4.5–5.1 €/kg) under the considered scenarios. This translated into a cost of CO_2 avoided between 90.1 €/tCO_2 and 115.5 €/tCO_2.

As shown in Figure 9a, the introduction of a gate fee of 40 €/t_{MSW} (Scenario 2) reduced the LCOH by 20.5% and 11% in case of conventional steam gasification and SEG, respectively. However, as the gate fee was introduced for both technologies, the cost of CO_2 avoided remained the same, around 115 €/tCO_2. This implies that consideration of the gate fee will not incentivise investment in SEG over the conventional steam gasification. On the contrary, introduction of the CO_2 emission allowance price (Scenario 3) has increased the LCOH of conventional steam gasification by 20.1% (from 2.7 €/kg to 3.2 €/kg), whereas the LCOH of SEG did increase by less than 0.8% (from 5.0 €/kg to 5.1 €/kg). This can be attributed to the lower CO_2 emitted in the latter case, since 90% of CO_2 emissions were captured in the carbonator. It is clear from Figure 9b that the introduction of the CO_2 emission allowance price had a large impact on the CO_2 avoided cost, reducing it by 21.5% with respect to Scenario 1.

Finally, the simultaneous introduction of the gate fee and the tax levied on fossil CO_2 emissions (Scenario 4) did not influence the LCOH for the conventional steam gasification, which remained at 2.7 €/kg. This implies that the reduction in the LCOH as a result of the introduction of the gate fee is

balanced by the increase in the LCOH due to the tax levied on the fossil CO_2 emissions. For SEG, however, the LCOH reduced by 10.2% under Scenario 4. The CO_2 avoided cost estimated for Scenario 4 was 90.8 €/tCO_2, which corresponds to a decrease of 21% with respect to baseline Scenario 1. Although SEG is not yet economically competitive with the conventional steam gasification, the results presented in this study demonstrated that SEG can become the preferred option when the EUA price exceeds 183 €/tCO_2. Even though the costs of CO_2 avoided associated with MSW gasification with CO_2 capture and SEG are not available, the figures estimated in this study are comparable with that reported for the steam-methane reforming (15.3–127.0 €/tCO_2), but almost the double of that reported for coal gasification (16.1–61.4 €/tCO_2). This can be explained by the large scale of plants considered in these studies as well as the low costs of feedstock [73].

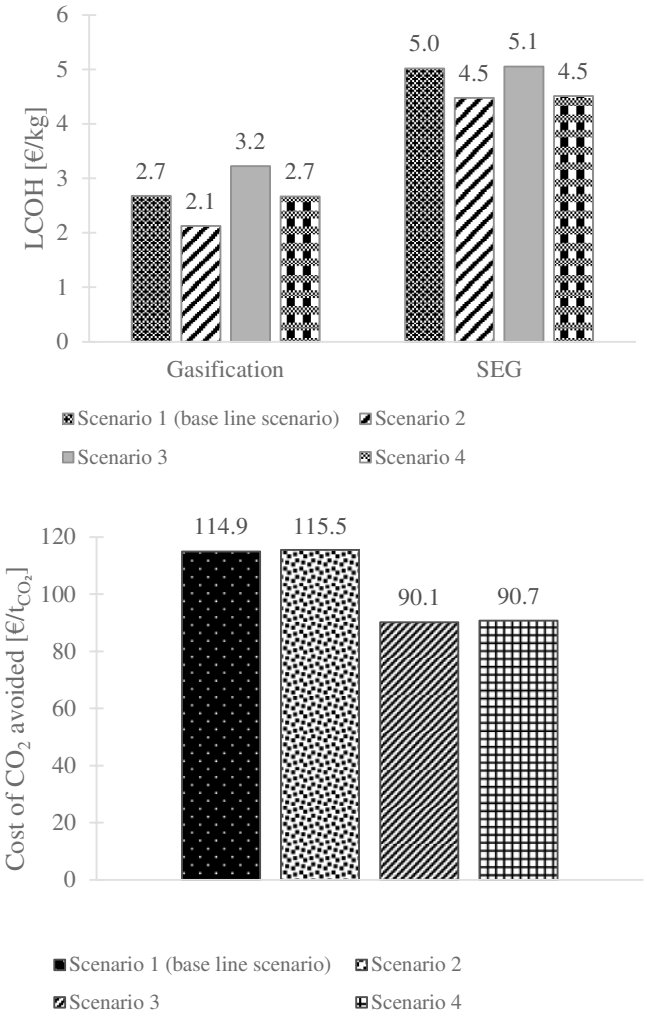

Figure 9. Comparison of levelised cost of hydrogen for gasification and sorption enhanced gasification plant, with and without a gate fee and CO_2 allowance price of 40 €/t_{MSW} and 39.6 €/tCO_2, respectively.

4.3. Sensitivity study

As shown above, the technical and economic assumptions, such as the plant capacity, fuel price, capital cost or a gate fee, are associated with uncertainty that can influence the economic results. Therefore, a sensitivity analysis was carried out to understand the effect of the main input variables in the economic model on the cost of CO_2 avoided. The capital costs of conventional steam gasification and SEG, as well as the price of limestone, electricity and CO_2 transport and storage were varied by ±25%.

The results presented in Figure 10 show that the uncertainty in the capital cost had the highest impact on the CO_2 avoided cost. Namely, a 25% reduction in the capital cost of SEG was shown to result in a 47% reduction in the cost of CO_2 avoided, assuming that the capital cost of conventional steam gasification remained fixed. On the contrary, if the capital cost of the conventional steam gasification increased 25% while the SEG cost remained unchanged, the CO_2 avoided cost would reduce by 30.5%. This indicates that even small reduction in the capital cost of SEG can significantly improve its economic viability. Furthermore, the variation in the electricity and limestone prices had shown a marginal impact on cost of CO_2 avoided. The ±25% variation in these parameters resulted only in ±1.6% and ±0.6% change in the cost of CO_2 avoided, respectively. Finally, a 25% increase in the cost associated with the CO_2 transport and storage was shown to result in a 5% increase in the cost of CO_2 avoided. Therefore, further work should focus on reducing the capital cost of SEG.

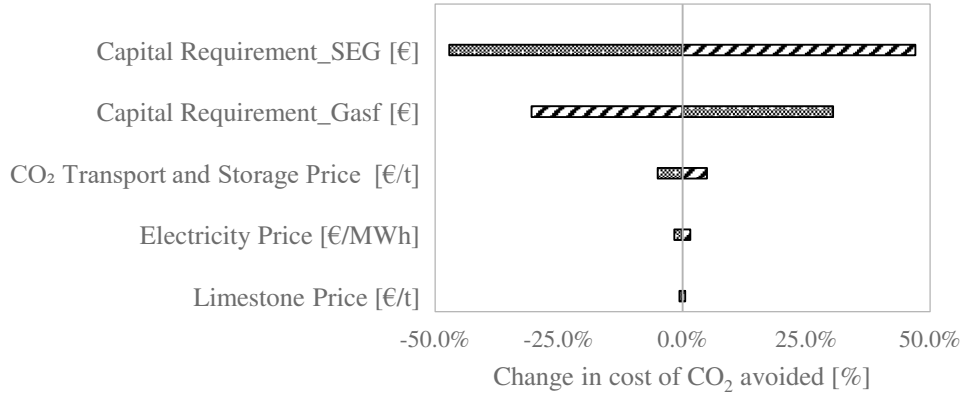

Figure 10. Effect of the main economic parameters on the cost of CO_2 avoided. Stripes: +25% of baseline parameter, Bubbles: -25% of baseline parameter

5. Technology benchmarks

The techno-economic performance of SEG was benchmarked against the conventional steam gasification, the comparison is shown in Table 8. The equivalent CO_2 emissions, estimated by Eq. 10, were used as an environmental indicator to compare the environmental performance of SEG and conventional steam gasification (Table 8). As can be seen, the equivalent CO_2 emissions were reduced from 21.7 $\mathbf{kg_{CO_2}/kg_{H_2}}$ (conventional steam gasification) to 1.4 $\mathbf{kg_{CO_2}/kg_{H_2}}$ (sorption enhanced gasification). In future works, this analysis should be carried out using advanced sustainability

assessment tools such as life cycle assessment, exergy analysis and the combination of the latter with economic and environmental analysis, exergoenvironmental and exergoeconomic analyses [74].

Table 8. Summary of techno-economic performance for both technologies

Parameter	Conventional steam gasification	Sorption enhanced gasification
Thermodynamic assessment		
H_2 production efficiency [%]	47.7	48.7
Gross power efficiency [%]	18.9	17.0
Net power efficiency [%]	6.0	0.6
Total power efficiency [%]	53.3	49.3
Environmental assessment		
Equivalent CO_2 emissions [kg_{CO_2}/kg_{H_2}]	21.7	1.4
Economic assessment		
Levelised cost of H_2 [€/kg]	2.7	5.0
Cost of CO_2 avoided [€/tCO_2]	-	114.9

A comparison between the LCOH estimated in this study and the LCOH reported in the literature for different technologies is shown in Figure 11.

Currently, steam-methane reforming (SMR) is the most commonly used and the cheapest technology for hydrogen production at scale, although its economic viability is very sensitive to the natural gas price. For this technology, the LCOH falls in the range between 1.0–1.5 €/kg without CO_2 capture and between 1.1 and 2.6 €/kg with CO_2 capture [73]. It can be seen in Figure 11 that coal gasification is also a competitive route for hydrogen production. While the LCOH for the processes without CO_2 capture varies between 0.9 €/kg and 1.8 €/kg, the integration of CO_2 capture results in a 33–94% increase in the LCOH (1.2–3.4 €/kg) [73]. Another route to produce hydrogen using renewable energy is biomass gasification. Yet, it is not a competitive technology at the current stage of development. The LCOH reported in the literature falls between 1.4 €/kg and 3.2 €/kg without CO_2 capture and between 2.1 €/kg and 3.3 €/kg with CO_2 capture [73,75]. It should be noted that there is a limited number of economic assessments for this technology in the current literature and, therefore, the latter figures are based only on the studies by Parkinson et al [73] and Salkuyeh et al. [75]. Shahabuddin et al. [76] were the first to estimate the LCOH for the MSW gasification without CO_2 capture. In their preliminary study, they found that the LCOH depended on the plant capacity and the consideration of a gate fee of around 45 €/t_{MSW}. The LCOH ranged from 2.4 €/kg (with gate fee) to 4.5 €/kg (without gate fee) for a plant of 75 MW_{th}. An increase of the plant capacity to 150 MW_{th} was shown to reduce the LCOH to between 1.3–3.5 €/kg. The economic feasibility of biomass SEG, at the plant capacity of

70 MW_{th}, was studied as a hydrogen production alternative by Schweitzer et al. [36]. They estimated the LCOH of between 6.1 and 10.1 €/kg, which were assessed for a capital cost between 1000 €/kW_{th} and 2000 €/kW_{th}.

The LCOH estimated in this study for a 100 MW_{th} MSW gasification plant without CO_2 capture (2.0–3.4 €/kg) is comparable with the figures reported above. Regarding the MSW SEG, The LCOH found in this work (3.9–6.1 €/kg) is lower than the values reported for biomass SEG by Schweitzer et al. [36]. This which can be primarily explained by no fuel cost associated with the use of MSW and the higher capacity of the SEG assumed in this work (100 MW_{th}).

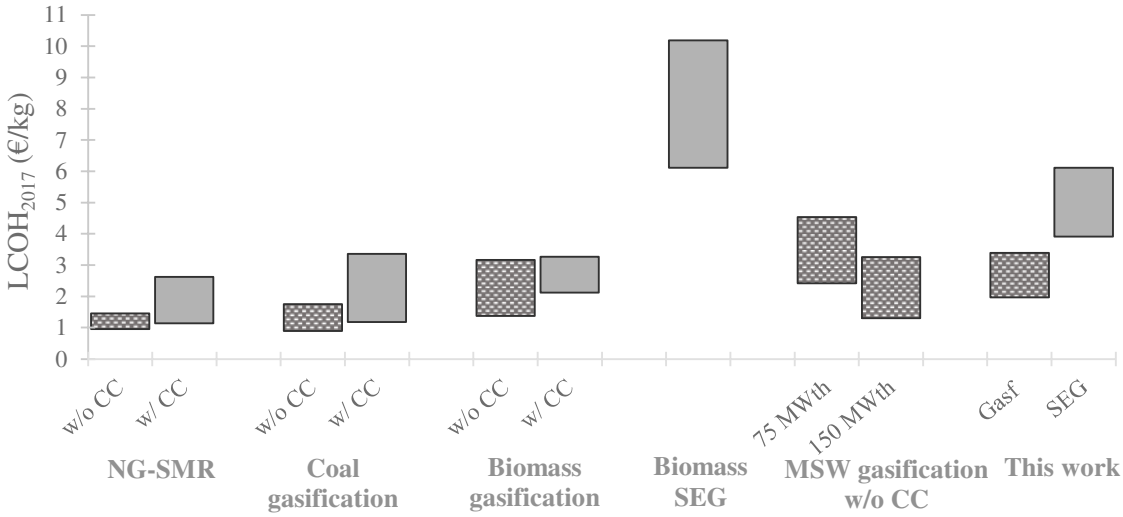

Figure 11. Levelised cost of hydrogen estimated for different technologies. Data from [36,73,75,76]**. Values for biomass sorption enhanced gasification based on the sensitivity analysis of capital cost. Values for municipal solid waste based on application of gate fee for different size plant.**

6. Conclusions

Waste-to-fuel conversion is a promising technology to simultaneously tackle the climate change and reduce the waste landfilling. In this work, the techno-economic performance of the MSW steam gasification without CO_2 capture and SEG, which comprises in-situ CO_2 capture, was compared. The LCOH was one of the key economic indicators to assess the economic performance of the considered gasification technologies. The cost associated with CO_2 capture, defined by the cost of CO_2 avoided, was also determined. It was shown that SEG can deliver a higher H_2 production efficiency than the conventional steam gasification. Depending on the operating conditions, the improvement in H_2 production efficiency can reach almost 4 percentual points. However, considering the optimal conditions of both technologies, the total efficiency delivered by SEG was 49.3% compared to 53.3% for the conventional steam gasification. This can be explained by the energy penalty associated with the CO_2 capture. Under the baseline scenario, the LCOH of 2.7 €/kg and 5.0 €/kg was estimated for MSW steam gasification and SEG, respectively. This corresponded to a cost of CO_2 avoided of 114.9 €/tCO_2. Although the integration of CO_2 capture resulted in an economic penalty, the cost of CO_2

avoided can be lowered by around 20% (90.1 €/tCO_2) if a CO_2 emission allowance price of 39.6 €/tCO_2 is levied to the fossil CO_2 emissions. Overall, the LCOH estimated for the MSW SEG was lower than the figures reported for biomass SEG and the cost of CO_2 avoided was in the range for steam-methane reforming, indicating the potential of SEG to produce low-carbon H_2. As the economic analysis was associated with a high uncertainty, a sensitivity analysis was carried out. The results indicated the capital cost of both technologies had the highest impact on the cost of CO_2 avoided. The sensitivity study showed that the cost of CO_2 avoided can be reduced by 47% and 30.5% if the capital cost of SEG decreased by 25% and the capital cost of gasification increased by 25%, respectively.

Although the LCOH was shown to be lower for more technologies, such as natural gas SMR or coal gasification, SEG can become a competitive technology in the future. This can be primarily achieved by considering advanced reactors to reduce the capital cost. Moreover, the recent forecasts of the EUA prices indicate that it will increase in the next decades, promoting application of low-carbon technologies such as SEG.

It is noteworthy this study research presents some limitations that need to be address in future research. A quasi-equilibrium approach was adopted to model the gasification. This model does not account the tar formation and the reaction kinetics. However, this limitation can be overcome in future work by adopting a kinetic based model and considering the bed hydrodynamics. The performance of the system was evaluated only from a thermodynamic and economic point of view. Besides, the energy analysis was based on the first law of thermodynamics, which does not consider the irreversibility of system. Therefore, the future work on the H_2 production systems should be simultaneously assessed under a thermodynamic, economic and environmental perspective.

Acknowledgements

This publication is based on research conducted within the "Clean heat, power and hydrogen from biomass and waste" project funded by UK Engineering and Physical Sciences Research Council (EPSRC reference: EP/R513027/1).

Nomenclature

A_j	heat exchanger area of equipment j [m^2]
AC	cost of CO_2 avoided [€/tCO_2]
ASU	air separation unit
BFB	bubbling fluidised bed
C_j	capital cost of equipment j [€]
CaL	calcium looping
CCS	carbon capture and storage
$CEPCI$	Chemical Engineering Plant Cost Index
CF_t	discounted cash flows through the project lifetime [€]

COS	carbonyl sulphide reactor
DFB	dual fluidised bed
$\boldsymbol{e_{CO_2}}$	direct CO_2 emissions from the plant [$\mathbf{kg_{CO_2}/kg_{H_2}}$]
$\boldsymbol{e_{CO_2,e}}$	specific CO_2 emissions associated with power generation [$\mathbf{kg_{CO_2}}$/$MW_{el}h$]
$\boldsymbol{e_{CO_2,eq}}$	equivalent CO_2 emissions [$\mathbf{kg_{CO_2}/kg_{H_2}}$]
ETS	Emissions Trading System
EUA	CO_2 emission allowance
EPC	engineering procurement and construction [€]
GHG	greenhouse gas
HTS	high-temperature shift reactor
LCOH	levelised cost of hydrogen [€/kg]
LHV	lower heating value [MJ/kg]
LO-CAT	liquid oxidation catalyst
LTS	low-temperature shift reactor
$\boldsymbol{\dot{m}_i}$	flowrate of component i [kg/s] or [t/h] or [kg/h]
MSW	municipal solid waste
NPV	net present value [€]
OCAPEX	other capital cost [€]
P_e	specific energy [$MW_{el}h$**/**$\mathbf{kg_{H_2}}$]
PC	project contingency [€]
PSA	pressure swing adsorption
r	discount rate [%]
SBR	steam-to-biomass ratio [kg/kg]
S/C	molar steam-to-carbon [mol/mol]
SEG	sorption enhanced gasification
SMR	steam methane reforming
t	project lifetime [y]
T	temperature [°C]
TCR	total capital requirement [€]
TIC	total installed cost [€]
TPC	total plant cost [€]
$\boldsymbol{W_{el,gross}}$	gross electric power output [MW_{el}]
$\boldsymbol{W_{el,net}}$	net electric power output [MW_{el}]
$\dot{W}_j$	brake power requirement/output of equipment j [kW_{el}]
WGS	water gas shift
WTE	waste-to-energy

ZnO	zinc oxide bed

Greek letters

η_{H_2}	H_2 production efficiency
$\eta_{el,gross}$	gross power efficiency
$\eta_{el,net}$	net power efficiency
$\eta_{el,net}$	total efficiency

Subscripts

0	reference value
AXPH	air preheater
ASU	air separation unit
BRKP	brake power
calc	calciner
CCU	CO_2 compression unit
COND	condensate
CW	fresh water
DEA	deaerator
eq	equivalent
ECON	economiser
FC	fuel compressor
Gasf	conventional steam gasification
GT	gas turbine
HPST	high-pressure steam turbine
HPW	high-pressure water
HRSG	heat recovery steam generator
IPST	intermediate-pressure steam turbine
LPST	low-pressure steam turbine
LPW	low-pressure water
LS	live steam
OXPH	oxygen preheater

[1] Kaza S, Yao LC., Bhada-Tata P, Van Woerden F. What a Waste 2.0 : A Global Snapshot of Solid Waste Management to 2050. Washington, DC: Urban Development;. Washington, DC: World Bank.; 2018.

[2] Hameed Z, Aslam M, Khan Z, Maqsood K, Atabani AE, Ghauri M, et al. Gasification of

municipal solid waste blends with biomass for energy production and resources recovery: Current status, hybrid technologies and innovative prospects. Renewable and Sustainable Energy Reviews 2021;136:110375. https://doi.org/10.1016/j.rser.2020.110375.

[3] Affairs D for EF& R. Uk Statistics on Waste. 2020. https://doi.org/10.1044/leader.ppl.25032020.24.

[4] Statista. Greenhouse gas emissions from landfill in the UK 2010-2019 2021. https://www.statista.com/statistics/509129/greenhouse-gas-emissions-landfill-in-the-united-kingdom-uk/ (accessed January 27, 2021).

[5] Tursi A. A review on biomass: Importance, chemistry, classification, and conversion. Biofuel Research Journal 2019;6:962–79. https://doi.org/10.18331/BRJ2019.6.2.3.

[6] Parthasarathy P, Narayanan KS. Hydrogen production from steam gasification of biomass: Influence of process parameters on hydrogen yield – A review. Renewable Energy 2014;66:570–9. https://doi.org/10.1016/j.renene.2013.12.025.

[7] Kırtay E. Recent advances in production of hydrogen from biomass. Energy Conversion and Management 2011;52:1778–89. https://doi.org/10.1016/j.enconman.2010.11.010.

[8] Chen G, Jamro IA, Samo SR, Wenga T, Baloch HA, Yan B, et al. Hydrogen-rich syngas production from municipal solid waste gasification through the application of central composite design: An optimization study. International Journal of Hydrogen Energy 2020;45:33260–73. https://doi.org/10.1016/j.ijhydene.2020.09.118.

[9] Meng F, Meng J, Zhang D. Influence of higher equivalence ratio on the biomass oxygen gasification in a pilot scale fixed bed gasifier. Journal of Renewable and Sustainable Energy 2018;10:053101. https://doi.org/10.1063/1.5040130.

[10] Fremaux S, Beheshti S-M, Ghassemi H, Shahsavan-Markadeh R. An experimental study on hydrogen-rich gas production via steam gasification of biomass in a research-scale fluidized bed. Energy Conversion and Management 2015;91:427–32. https://doi.org/10.1016/j.enconman.2014.12.048.

[11] Zheng X, Ying Z, Wang B, Chen C. Hydrogen and syngas production from municipal solid waste (MSW) gasification via reusing CO2. Applied Thermal Engineering 2018;144:242–7. https://doi.org/10.1016/j.applthermaleng.2018.08.058.

[12] Udomsirichakorn J, Salam PA. Review of hydrogen-enriched gas production from steam gasification of biomass: The prospect of CaO-based chemical looping gasification. Renewable and Sustainable Energy Reviews 2014;30:565–79. https://doi.org/10.1016/j.rser.2013.10.013.

[13] Arregi A, Amutio M, Lopez G, Bilbao J, Olazar M. Evaluation of thermochemical routes for hydrogen production from biomass: A review. Energy Conversion and Management 2018;165:696–719. https://doi.org/10.1016/j.enconman.2018.03.089.

[14] Zhang S, Yin H, Wang J, Zhu S, Xiong Y. Catalytic cracking of biomass tar using Ni nanoparticles embedded carbon nanofiber/porous carbon catalysts. Energy 2021;216:119285. https://doi.org/10.1016/j.energy.2020.119285.

[15] Umar A, Neagu D, Irvine JTS. Alkaline modified A-site deficient perovskite catalyst surface with exsolved nanoparticles and functionality in biomass valorisation. Biofuel Research Journal 2021;8:1342–50. https://doi.org/10.18331/BRJ2021.8.1.5.

[16] Jordan CA, Akay G. Effect of CaO on tar production and dew point depression during gasification of fuel cane bagasse in a novel downdraft gasifier. Fuel Processing Technology 2013;106:654–60. https://doi.org/10.1016/j.fuproc.2012.09.061.

[17] Jordan CA, Akay G. Occurrence, composition and dew point of tars produced during gasification of fuel cane bagasse in a downdraft gasifier. Biomass and Bioenergy 2012;42:51–8. https://doi.org/10.1016/j.biombioe.2012.03.014.

[18] He C, Zheng J, Wang K, Lin H, Wang JY, Yang Y. Sorption enhanced aqueous phase reforming of glycerol for hydrogen production over Pt-Ni supported on multi-walled carbon nanotubes. Applied Catalysis B: Environmental 2015;162:401–11. https://doi.org/10.1016/j.apcatb.2014.07.012.

[19] Perejón A, Romeo LM, Lara Y, Lisbona P, Martínez A, Valverde JM. The Calcium-Looping technology for CO2 capture: On the important roles of energy integration and sorbent behavior. Applied Energy 2016;162:787–807. https://doi.org/10.1016/j.apenergy.2015.10.121.

[20] Li B, Yang H, Wei L, Shao J, Wang X, Chen H. Absorption-enhanced steam gasification of biomass for hydrogen production: Effects of calcium-based absorbents and NiO-based catalysts on corn stalk pyrolysis-gasification. International Journal of Hydrogen Energy 2017;42:5840–8. https://doi.org/10.1016/j.ijhydene.2016.12.031.

[21] Li B, Fabrice Magoua Mbeugang C, Liu D, Zhang S, Wang S, Wang Q, et al. Simulation of sorption enhanced staged gasification of biomass for hydrogen production in the presence of calcium oxide. International Journal of Hydrogen Energy 2020;45:26855–64. https://doi.org/10.1016/j.ijhydene.2020.07.121.

[22] Khan Z, Yusup S, Ahmad MM, Chin BLF. Hydrogen production from palm kernel shell via integrated catalytic adsorption (ICA) steam gasification. Energy Conversion and Management 2014;87:1224–30. https://doi.org/10.1016/j.enconman.2014.03.024.

[23] Acharya B, Dutta A, Basu P. Gasification of biomass in a circulating fluidized bed based calcium looping gasifier for hydrogen-enriched gas production: experimental studies. Biofuels 2017;8:643–50. https://doi.org/10.1080/17597269.2015.1118782.

[24] Acharya B, Dutta A, Basu P. An investigation into steam gasification of biomass for hydrogen enriched gas production in presence of CaO. International Journal of Hydrogen Energy 2010;35:1582–9. https://doi.org/10.1016/j.ijhydene.2009.11.109.

[25] Chen S, Zhao Z, Soomro A, Ma S, Wu M, Sun Z, et al. Hydrogen-rich syngas production via sorption-enhanced steam gasification of sewage sludge. Biomass and Bioenergy 2020;138:105607. https://doi.org/10.1016/j.biombioe.2020.105607.

[26] Detchusananard T, Im-orb K, Maréchal F, Arpornwichanop A. Analysis of the sorption-enhanced chemical looping biomass gasification process: Performance assessment and optimization through design of experiment approach. Energy 2020;207:118190. https://doi.org/10.1016/j.energy.2020.118190.

[27] Pitkäoja A, Ritvanen J, Hafner S, Hyppänen T, Scheffknecht G. Simulation of a sorbent enhanced gasification pilot reactor and validation of reactor model. Energy Conversion and Management 2020;204:112318. https://doi.org/10.1016/j.enconman.2019.112318.

[28] Martínez I, Kulakova V, Grasa G, Murillo R. Experimental investigation on sorption enhanced gasification (SEG) of biomass in a fluidized bed reactor for producing a tailored syngas. Fuel 2020;259:116252. https://doi.org/10.1016/j.fuel.2019.116252.

[29] He M, Xiao B, Liu S, Guo X, Luo S, Xu Z, et al. Hydrogen-rich gas from catalytic steam gasification of municipal solid waste (MSW): Influence of steam to MSW ratios and weight hourly space velocity on gas production and composition. International Journal of Hydrogen Energy 2009;34:2174–83. https://doi.org/10.1016/j.ijhydene.2008.11.115.

[30] Zhou C, Stuermer T, Gunarathne R, Yang W, Blasiak W. Effect of calcium oxide on high-temperature steam gasification of municipal solid waste. Fuel 2014;122:36–46. https://doi.org/10.1016/j.fuel.2014.01.029.

[31] Hu M, Guo D, Ma C, Hu Z, Zhang B, Xiao B, et al. Hydrogen-rich gas production by the gasification of wet MSW (municipal solid waste) coupled with carbon dioxide capture. Energy 2015;90:857–63. https://doi.org/10.1016/j.energy.2015.07.122.

[32] Irfan M, Li A, Zhang L, Wang M, Chen C, Khushk S. Production of hydrogen enriched syngas from municipal solid waste gasification with waste marble powder as a catalyst. International Journal of Hydrogen Energy 2019;44:8051–61. https://doi.org/10.1016/j.ijhydene.2019.02.048.

[33] Martínez I, Grasa G, Callén MS, López JM, Murillo R. Optimised production of tailored syngas from municipal solid waste (MSW) by sorption-enhanced gasification. Chemical Engineering Journal 2020;401:126067. https://doi.org/10.1016/j.cej.2020.126067.

[34] Müller S, Fuchs J, Schmid JC, Benedikt F, Hofbauer H. Experimental development of sorption enhanced reforming by the use of an advanced gasification test plant. International Journal of Hydrogen Energy 2017;42:29694–707. https://doi.org/10.1016/j.ijhydene.2017.10.119.

[35] Hawthorne C, Poboss N, Dieter H, Gredinger A, Zieba M, Scheffknecht G. Operation and results of a 200-kWth dual fluidized bed pilot plant gasifier with adsorption-enhanced reforming. Biomass Conversion and Biorefinery 2012;2:217–27. https://doi.org/10.1007/s13399-012-0053-3.

[36] Schweitzer D, Albrecht FG, Schmid M, Beirow M, Spörl R, Dietrich R-U, et al. Process simulation and techno-economic assessment of SER steam gasification for hydrogen production. International Journal of Hydrogen Energy 2018;43:569–79. https://doi.org/10.1016/j.ijhydene.2017.11.001.

[37] Wang J, Cheng G, You Y, Xiao B, Liu S, He P, et al. Hydrogen-rich gas production by steam gasification of municipal solid waste (MSW) using NiO supported on modified dolomite. International Journal of Hydrogen Energy 2012;37:6503–10. https://doi.org/10.1016/j.ijhydene.2012.01.070.

[38] Russo S, de Oliveira S, Desideri U. Thermo-economic evaluation of cogeneration plants based on municipal solid waste gasification in the Brazilian scenario. ECOS 2018 - Proceedings of the 31st International Conference on Efficiency, Cost, Optimization, Simulation and Environmental Impact of Energy Systems 2018.

[39] Arteaga-Pérez LE, Casas-Ledón Y, Pérez-Bermúdez R, Peralta LM, Dewulf J, Prins W. Energy and exergy analysis of a sugar cane bagasse gasifier integrated to a solid oxide fuel cell based on a quasi-equilibrium approach. Chemical Engineering Journal 2013;228:1121–32. https://doi.org/10.1016/j.cej.2013.05.077.

[40] Luz FC, Rocha MH, Lora EES, Venturini OJ, Andrade RV, Leme MMV, et al. Techno-economic analysis of municipal solid waste gasification for electricity generation in Brazil. Energy Conversion and Management 2015;103:321–37. https://doi.org/10.1016/j.enconman.2015.06.074.

[41] Doherty W, Reynolds A, Kennedy D. Aspen plus simulation of biomass gasification in a steam blown dual fluidised bed. Materials and Process for Energy 2013:212–20.

[42] NREL. Biomass to Hydrogen Production Detailed Design and Economics Utilizing the

Battelle Columbus Laboratory Indirectly-Heated Gasifier. 2005.

[43] NETL. Cost and performance baseline for fossil energy plants. Volume 1: Bituminous coal and natural gas to electricity. 2019.

[44] Marcantonio V, De Falco M, Capocelli M, Bocci E, Colantoni A, Villarini M. Process analysis of hydrogen production from biomass gasification in fluidized bed reactor with different separation systems. International Journal of Hydrogen Energy 2019;44:10350–60. https://doi.org/10.1016/j.ijhydene.2019.02.121.

[45] Materazzi M, Taylor R, Cairns-Terry M. Production of biohydrogen from gasification of waste fuels: Pilot plant results and deployment prospects. Waste Management 2019;94:95–106. https://doi.org/10.1016/j.wasman.2019.05.038.

[46] Santos MPS, Manovic V, Hanak DP. Unlocking the potential of pulp and paper industry to achieve carbon-negative emissions via calcium looping retrofit. Journal of Cleaner Production 2021;280:124431. https://doi.org/10.1016/j.jclepro.2020.124431.

[47] Romano MC. Ultra-high CO2 capture efficiency in CFB oxyfuel power plants by calcium looping process for CO2 recovery from purification units vent gas. International Journal of Greenhouse Gas Control 2013;18:57–67. https://doi.org/10.1016/j.ijggc.2013.07.002.

[48] Metz B, Davidson O, de Coninck H, Loos M, Meyer L. Carbon Dioxide Capture and Storage. Cambridge; New York; Melbourne; Madrid; Cape Town; Singapore; Sào Paulo: Cambridge University Press; 2005.

[49] Luberti M, Friedrich D, Brandani S, Ahn H. Design of a H2 PSA for cogeneration of ultrapure hydrogen and power at an advanced integrated gasification combined cycle with pre-combustion capture. Adsorption 2014;20:511–24. https://doi.org/10.1007/s10450-013-9598-0.

[50] Hu M. The New SeparALLTM Process and PolybedTM PSA for IGCC and CTL Application. 7th International Freiberg Conference Hohhot, China, June 7th-11th, 2015.

[51] Armbrust N, Duelli G, Dieter H, Scheffknecht G. Calcium looping cycle for hydrogen production from biomass gasification syngas: Experimental investigation at a 20 kWth dual fluidized-bed facility. Industrial and Engineering Chemistry Research 2015;54:5624–34. https://doi.org/10.1021/acs.iecr.5b00070.

[52] Hanak DP, Manovic V. Combined heat and power generation with lime production for direct air capture. Energy Conversion and Management 2018;160:455–66. https://doi.org/10.1016/j.enconman.2018.01.037.

[53] Spallina V, Motamedi G, Gallucci F, van Sint Annaland M. Techno-economic assessment of

an integrated high pressure chemical-looping process with packed-bed reactors in large scale hydrogen and methanol production. International Journal of Greenhouse Gas Control 2019;88:71–84. https://doi.org/10.1016/j.ijggc.2019.05.026.

[54] Onarheim K, Santos S, Kangas P, Hankalin V. Performance and cost of CCS in the pulp and paper industry part 2: Economic feasibility of amine-based post-combustion CO2 capture. International Journal of Greenhouse Gas Control 2017;66:60–75. https://doi.org/10.1016/j.ijggc.2017.09.010.

[55] Maas W. The post-2020 Cost-Competitiveness of CCS Cost of Storage. n.d.

[56] Martínez A, Lara Y, Lisbona P, Romeo LM. Operation of a mixing seal valve in calcium looping for CO2 capture. Energy and Fuels 2014;28:2059–68. https://doi.org/10.1021/ef402487e.

[57] Yang Y, Zhai R, Duan L, Kavosh M, Patchigolla K, Oakey J. Integration and evaluation of a power plant with a CaO-based CO2 capture system. International Journal of Greenhouse Gas Control 2010;4:603–12. https://doi.org/10.1016/j.ijggc.2010.01.004.

[58] Bank of England. Bank of England Statistical Interactive Database | Interest & Exchange Rates | Official Bank Rate History 2019. http://www.bankofengland.co.uk/boeapps/iadb/repo.asp (accessed December 5, 2019).

[59] Ember. Daily Carbon Prices 2021. https://ember-climate.org/data/carbon-price-viewer/.

[60] Haaf M, Ohlemüller P, Ströhle J, Epple B. Techno-economic assessment of alternative fuels in second-generation carbon capture and storage processes. Mitigation and Adaptation Strategies for Global Change 2020;25:149–64. https://doi.org/10.1007/s11027-019-09850-z.

[61] De Lena E, Spinelli M, Gatti M, Scaccabarozzi R, Campanari S, Consonni S, et al. Techno-economic analysis of calcium looping processes for low CO2 emission cement plants. International Journal of Greenhouse Gas Control 2019;82:244–60. https://doi.org/10.1016/j.ijggc.2019.01.005.

[62] NREL. Process Design and Economics for Conversion of Lignocellulosic Biomass to Ethanol: Thermochemical Pathway by Indirect Gasification and Mixed Alcohol Synthesis. 2011.

[63] Spallina V, Pandolfo D, Battistella A, Romano MC, Van Sint Annaland M, Gallucci F. Techno-economic assessment of membrane assisted fluidized bed reactors for pure H2 production with CO2 capture. Energy Conversion and Management 2016;120:257–73. https://doi.org/10.1016/j.enconman.2016.04.073.

[64] Michalski S, Hanak DP, Manovic V. Techno-economic feasibility assessment of calcium

looping combustion using commercial technology appraisal tools. Journal of Cleaner Production 2019;219:540–51. https://doi.org/10.1016/j.jclepro.2019.02.049.

[65] Atsonios K, Koumanakos A, Panopoulos KD, Doukelis A, Kakaras E. Techno-economic comparison of CO2 capture technologies employed with natural gas derived GTCC. Proceedings of the ASME Turbo Expo, vol. 2, 2013, p. V002T07A018. https://doi.org/10.1115/GT2013-95117.

[66] Kreutz T, Williams R, Consonni S, Chiesa P. Co-production of hydrogen, electricity and CO from coal with commercially ready technology. Part B: Economic analysis. International Journal of Hydrogen Energy 2005;30:769–84. https://doi.org/10.1016/j.ijhydene.2004.08.001.

[67] Lee YD, Ahn KY, Morosuk T, Tsatsaronis G. Exergetic and exergoeconomic evaluation of a solid-oxide fuel-cell-based combined heat and power generation system. Energy Conversion and Management 2014;85:154–64. https://doi.org/10.1016/j.enconman.2014.05.066.

[68] Shirazi A, Aminyavari M, Najafi B, Rinaldi F, Razaghi M. Thermal–economic–environmental analysis and multi-objective optimization of an internal-reforming solid oxide fuel cell–gas turbine hybrid system. International Journal of Hydrogen Energy 2012;37:19111–24. https://doi.org/10.1016/j.ijhydene.2012.09.143.

[69] Manzolini G, Macchi E, Gazzani M. CO2 capture in natural gas combined cycle with SEWGS. Part B: Economic assessment. International Journal of Greenhouse Gas Control 2013;12:502–9. https://doi.org/10.1016/j.ijggc.2012.06.021.

[70] Sayyaadi H, Mehrabipour R. Efficiency enhancement of a gas turbine cycle using an optimized tubular recuperative heat exchanger. Energy 2012;38:362–75. https://doi.org/10.1016/j.energy.2011.11.048.

[71] Li W, Li Q, Chen R, Wu Y, Zhang Y. Investigation of hydrogen production using wood pellets gasification with steam at high temperature over 800 °c to 1435 °c. International Journal of Hydrogen Energy 2014;39:5580–8. https://doi.org/10.1016/j.ijhydene.2014.01.102.

[72] Rapagnà S, Jand N, Kiennemann A, Foscolo PU. Steam-gasification of biomass in a fluidised-bed of olivine particles. Biomass and Bioenergy 2000;19:187–97. https://doi.org/10.1016/S0961-9534(00)00031-3.

[73] Parkinson B, Balcombe P, Speirs JF, Hawkes AD, Hellgardt K. Levelized cost of CO2 mitigation from hydrogen production routes. Energy & Environmental Science 2019;12:19–40. https://doi.org/10.1039/C8EE02079E.

[74] Rosen MA. Environmental sustainability tools in the biofuel industry. Biofuel Research

Journal 2018;5:751–2. https://doi.org/10.18331/BRJ2018.5.1.2.

[75] Salkuyeh YK, Saville BA, MacLean HL. Techno-economic analysis and life cycle assessment of hydrogen production from different biomass gasification processes. International Journal of Hydrogen Energy 2018;43:9514–28. https://doi.org/10.1016/j.ijhydene.2018.04.024.

[76] Shahabuddin M, Krishna BB, Bhaskar T, Perkins G. Advances in the thermo-chemical production of hydrogen from biomass and residual wastes: Summary of recent techno-economic analyses. Bioresource Technology 2020;299:122557. https://doi.org/10.1016/j.biortech.2019.122557.

Techno-economic feasibility assessment of sorption enhanced gasification of municipal solid waste for hydrogen production

Santos, Mónica P. S.

2022-01-13

Santos MPS, Hanak DP. (2022) Techno-economic feasibility assessment of sorption enhanced gasification of municipal solid waste for hydrogen production, International Journal of Hydrogen Energy, Volume 47, Issue 10, February 2022, pp. 6586-6604

https://doi.org/10.1016/j.ijhydene.2021.12.037